Dysregulated neuroimmune interactions and sustained type I interferon signaling after human immunodeficiency virus type 1 infection of human iPSC derived microglia and cerebral organoids

Andrew J. Boreland[1,2], Alessandro C. Stillitano[1], Hsin-Ching Lin[1], Yara Abbo[1], Ronald P. Hart[3], Peng Jiang[3], Zhiping P. Pang[1,2*], Arnold B. Rabson[1,4*]

[1] Child Health Institute of New Jersey, Rutgers Robert Wood Johnson Medical School, New Brunswick, NJ

[2] Department of Neuroscience, Rutgers Robert Wood Johnson Medical School, New Brunswick, NJ

[3] Department of Cell Biology and Neuroscience, Rutgers University, Piscataway, NJ

[4] Departments of Pharmacology, Pathology & Laboratory Medicine, and Pediatrics, Rutgers Robert Wood Johnson Medical School, New Brunswick, NJ

*Correspondence: zhiping.pang@rutgers.edu and rabsonab@rwjms.rutgers.edu

17 Highlights of the work:

18 - HIV-1 productively infects iPSC-derived microglia and triggers inflammatory activation.
19 - HIV-1 infection of microglia results in sustained type I interferon signaling.
20 - Microglia infected by HIV-1 incorporate into sliced neocortical organoids with persistent
21 type I interferon signaling and disease risk gene expression.

22

ABSTRACT

Human immunodeficiency virus type-1 (HIV-1) associated neurocognitive disorder (HAND) affects up to half of HIV-1 positive patients with long term neurological consequences, including dementia. There are no effective therapeutics for HAND because the pathophysiology of HIV-1 induced glial and neuronal functional deficits in humans remains enigmatic. To bridge this knowledge gap, we established a model simulating HIV-1 infection in the central nervous system using human induced pluripotent stem cell (iPSC) derived microglia combined with sliced neocortical organoids. Upon incubation with two replication-competent macrophage-tropic HIV-1 strains (JRFL and YU2), we observed that microglia not only became productively infected but also exhibited inflammatory activation. RNA sequencing revealed a significant and sustained activation of type I interferon signaling pathways. Incorporating microglia into sliced neocortical organoids extended the effects of aberrant type I interferon signaling in a human neural context. Collectively, our results illuminate the role of persistent type I interferon signaling in HIV-1 infected microglial in a human neural model, suggesting its potential significance in the pathogenesis of HAND.

INTRODUCTION

The global burden of human immunodeficiency virus-1 (HIV-1) infection remains profound, with neurocognitive complications manifesting in a significant proportion of infected individuals despite the remarkable success of combined antiretroviral therapy (cART) in reducing morbidity and mortality. Up to 55% of HIV-1 positive people experience neurological complications that may develop into HIV associated neurocognitive disorder (HAND) (Simioni et al. 2010; Sacktor et al. 2016; Eggers et al. 2017; Sacktor 2018). This debilitating disorder manifests across a spectrum of cognitive, motor, affective, and behavioral impairments, which can severely impact the quality of life for affected individuals, emphasizing an urgent need for a better understanding of its underlying mechanisms (Lew et al. 2018; Israel et al. 2019). The etiology and neuropathogenesis of HAND remain enigmatic, as there has been no evidence of neuronal HIV-1 infection. Decades of research suggest that HAND development is caused by a combination of both direct and indirect effects involving viral proteins, inflammatory cytokines and chemokines, and dysregulated neuroimmune interactions (Koenig et al. 1986; Gendelman et al. 1994; Rappaport et al. 1999; González-Scarano and Martín-García 2005; Kraft-Terry et al. 2009; Lindl et al. 2010; Burdo, Lackner, and Williams 2013; Alvarez-Carbonell et al. 2020). Interestingly, clinical symptoms of HAND correlate more closely with cytokine production, neuronal pathology, decreased synaptic density, and increased microglia than with central nervous system (CNS) viral load (Kaul, Garden, and Lipton 2001; Kaul et al. 2005). Currently there is a lack of mechanistic understanding due to a need for better experimental models that can address these questions, especially regarding neuroimmune interactions.

A pivotal component of neuroimmune interactions is the innate immune response, including the production and signaling of interferons, which have recently been implicated in the neuropathology of various neurological diseases [Reviewed in (Hofer and Campbell 2013; McGlasson et al. 2015)]. Interferons and their downstream signaling through interferon stimulated genes (ISGs) are primarily an innate immune response to viral infection [reviewed in (Platanias

65 2005)]. However, recent literature suggests a role for dysregulated type I interferon signaling in
66 neurological diseases such as Alzheimer's disease (Roy et al. 2020; Roy et al. 2022), COVID-19
67 related brain fog (Lee and Shin 2020; Phetsouphanh et al. 2022), aging associated dementia
68 (Baruch et al. 2014), and HIV associated dementia (Rho et al. 1995; Krivine et al. 1999; Perrella
69 et al. 2001; Anderson et al. 2017; Solomon et al. 2020). Clinically, type I interferons have been
70 shown to be a driver of cognitive impairment both in diseased states and when administered
71 exogenously (Merimsky et al. 1990). Indeed, many studies using interferon treatment for various
72 severe cancers and chronic viral hepatitis C have reported that patients receiving interferon-alpha
73 displayed cognitive, mood, and behavioral deficits that arose and worsened with prolonged,
74 multiweek treatment regimens (Christina, Randall, and Arthur 1991; Pavol et al. 1995; Capuron,
75 Ravaud, and Dantzer 2001; Capuron et al. 2002; Wichers et al. 2005; Raison et al. 2005). Taken
76 together, these studies indicate a role for aberrant type I interferon signaling in compromising
77 neuronal and glial function, leading to cognitive deficits and degeneration.

78 Microglia, as the resident immune cells of the CNS and the primary CNS target of HIV-1
79 infection, contribute significantly to the pathophysiology of HAND, largely through their secretory
80 and functional dysregulation. Under homeostatic conditions, microglia play important roles in
81 synaptic pruning, phagocytic functions, immune surveillance, and extracellular matrix remodeling
82 (Paolicelli et al. 2011; Casano and Peri 2015). When challenged, microglial activation can be
83 either neurotoxic, producing proinflammatory cytokines and chemokines, or neurotrophic,
84 producing anti-inflammatory cytokines (Durafourt et al. 2012). Microglia exhibit a heterogeneous
85 spectrum of activation and disease-associated states with unique properties and consequences
86 on neuronal functions (Gosselin et al. 2017; Song and Colonna 2018; Hammond et al. 2019).

87 Since HIV-1 specifically infects humans, the ability of traditional animal model organisms
88 to replicate the complex disease processes of HAND is inherently limited. HIV-1-Simian
89 immunodeficiency virus chimeras (SHIVs) have been studied in monkey models. However, these
90 models are limited in their availability and utility for molecular analyses [reviewed in (Byrnes et al.

91 2022; Moretti et al. 2021)]. Recent advances in stem cell technologies have opened up new
92 possibilities for modeling and studying HAND, particularly the development of human iPSC
93 derived neurons, astrocytes, and microglia capable of mimicking complex in vivo neuroimmune
94 interactions when grown in three dimensional cerebral organoid cultures (Abud et al. 2017; Ormel
95 et al. 2018; Xu et al. 2021). Cerebral organoids offer a powerful and physiologically relevant
96 platform to study complex neuroimmune interactions, but traditional organoid differentiation
97 protocols do not produce microglia. Recent studies have demonstrated the feasibility of infecting
98 iPSC-derived macrophages (Vaughan-Jackson et al. 2021) and microglia (Rai et al. 2020) with
99 HIV-1. Moreover, these infected microglia have been effectively cocultured in various model
100 systems, including human stem cell derived neural tricultures (Alvarez-Carbonell et al. 2020; Ryan
101 et al. 2020), primary neuron progenitor cell derived organoids (dos Reis et al. 2020), iPSC-derived
102 cerebral organoids (Gumbs et al. 2022), and a humanized mouse model (Min et al. 2023).
103 In this study, we hypothesized that by infecting iPSC-derived microglia with replication
104 competent HIV-1 and integrating them into sliced neocortical organoids, we could recapitulate
105 neuroimmune dysregulation related to HAND pathology. We demonstrate that HIV-1 infection of
106 iPSC-derived microglia leads to persistent activation of type I interferon signaling and microglial
107 activation in both microglial monocultures and in the context of cerebral organoids.
108
109

110 **RESULTS**

111 **Human microglia are efficiently generated from iPSCs**

112 To induce microglial differentiation, we used three iPSC lines and employed previous protocols
113 (Haenseler et al. 2017; Xu et al. 2021). To mimic in vivo microglial development from the yolk sac,
114 iPSC embryoid bodies were patterned toward a mesodermal yolk sac lineage that generates
115 primitive macrophage precursors (PMPs) after 3 weeks of culture (**Figure 1A**). The identity of the
116 PMPs was confirmed by immunocytochemistry against CD235, a marker for yolk sac (Claes, Van
117 den Daele, and Verfaillie 2018), and CD43, a marker for hematopoietic progenitor like cells
118 (Vodyanik, Thomson, and Slukvin 2006) (**Figure 1B**). Upon further maturation under the influence
119 of a colony stimulating factor 1 receptor (CSF1R) antagonist, interleukin 34 (IL-34), and
120 granulocyte maturation factor (GM-CSF), PMPs exhibit a more pronounced microglial phenotype.
121 This was evidenced by a significant increase in mRNA expression of the microglial markers
122 ionized calcium binding molecule 1 (IBA1) and purinergic receptor P2Y12 across all three cell
123 lines (**Figure 1C,** biological replicates of each cell line shown in **Figure S1**). Supporting these
124 gene expression results, we noted robust immunocytochemical staining of the microglial markers
125 IBA1, P2Y12, CX3CR1, transmembrane protein 119 (TMEM119), and transcription factor PU.1 in
126 maturing microglia from these same lines (**Figure 1D**). Upon coculture of microglia with iPSC-
127 derived neurons (Xu et al. 2021), we found that microglia display a more elaborate morphology
128 (**Figure 1E**). Furthermore, costaining with the neuronal dendritic marker microtubule-associated
129 protein 2 (MAP2) and the presynaptic marker synapsin 1 (SYN1) revealed that microglial
130 processes interact with dendrites and colocalize with synaptic puncta, indicating putative
131 microglia-synapse interactions (**Figure 1F**).

132 Given the tropism of HIV-1 for CD4 receptor expressing cells and the requirement of CCR5
133 coreceptor expression for infection of monocyte/macrophage related cell lineages, we assessed
134 the gene expression of *CD4* and *CCR5* in iPSC-derived microglia. Results showed significantly
135 increased mRNA expression of *CD4* and *CCR5* in microglia differentiated from all three iPSC

136 lines (**Figure 1G,** biological replicates of each cell line shown in **Figure S1**). These results
137 demonstrate that microglia can be successfully and reproducibly generated from iPSCs. Crucially,
138 these cells express appropriate markers for microglial identity and infection by HIV-1.
139

140 **iPSC derived microglia are productively infected by HIV-1 and exhibit inflammatory**
141 **activation**

142 Having confirmed the generation and maturation of iPSC-derived microglia, we next determined
143 whether these cells could sustain a productive infection by replication competent, macrophage
144 tropic HIV-1. To this end, we incubated male 03SF iPSC-derived microglia with JRFL HIV (2
145 ng/ml), an R5 tropic HIV-1 strain isolated from the cerebral spinal fluid (CSF) of a patient with
146 severe HAND (Koyanagi et al. 1987; Merrill et al. 1992). Compared to uninfected controls, HIV-
147 1-infected microglia robustly expressed HIV-1 *gag/pol* RNA within 6-9 days after infection (Yu et
148 al. 1996) (**Figure 2A**). As a key indicator of productive HIV-1 infection, the production of secreted
149 p24 was measured (Chargelegue and O'Toole 1992; Marodon et al. 1999). Using ELISA to detect
150 secreted p24 in the culture supernatant, we observed increased protein production starting 1
151 week post infection, peaking around day 16, and then maintaining consistent levels for more than
152 2 weeks (**Figure 2B**). Finally, we found that after just 4 days post infection, circular polymerase
153 chain reaction (PCR) products from both long terminal repeats (LTR) were detected in HIV-1
154 incubated cultures indicating the presence of active viral replication (Butler, Hansen, and
155 Bushman 2001) (**Figure S2**).

156 After establishing the infectability of iPSC microglia with HIV-1 JRFL, we then asked
157 whether HIV-1 infection elicits differential expression of inflammatory and canonical microglial
158 mRNAs using reverse transcription–quantitative PCR (RT-qPCR). In this second experiment
159 found we found HIV-1 infection augmented the expression of the inflammation-associated genes
160 interleukin 1ß (IL1ß, on day 16) and tumor necrosis factor alpha (TNFα), while the expression of

161 interleukin 6 (IL6) displayed no change (**Figure 2C**). We then examined the mRNA expression of
162 the chemokines CCL2 (monocyte chemoattractant protein 1, MCP-1), CCL3 (macrophage
163 inflammatory protein 1 alpha, MIP-1), and CCL5 (RANTES). These three chemokines play
164 important roles in immune cell recruitment and migration to sites of inflammation and infection
165 and have been found to be elevated in cognitively impaired individuals with HIV-1 (Letendre,
166 Lanier, and McCutchan 1999). A significant elevation in the mRNA expression of CCL2 and CCL3
167 was observed by day 16 post-infection, whereas the expression of CCL5 remained unchanged
168 (**Figure 2D**). To assess whether microglial identity was altered by HIV-1 infection, we assessed
169 the mRNA expression of the canonical microglial genes IBA1 and P2Y12. While IBA1 remained
170 stable, P2Y12 exhibited significantly increased expression by day 23 post infection (**Figure 2E**).
171 Next, we asked how HIV-1 infection might alter microglial chemokine and cytokine production.
172 Although the levels of most cytokines were below the detection threshold (**Table S1**), we noted a
173 significant surge in the secretion of chemokines M-CSF and interferon inducible protein 10 (IP-
174 10/CXCL10) following HIV-1 infection in the same supernatant used in figure 2B (**Figure 2F**).
175 Finally, to visualize HIV-1 infected cells, we detected HIV-1 p24 protein using a biotin-streptavidin
176 amplification protocol (Eugenin and Berman 2016). On day 13 post infection with JRFL, p24
177 positive microglia were found (**Figure 2G**). Collectively, our findings suggest that iPSC-derived
178 microglia can sustain an R5 tropic HIV-1 infection and exhibit an inflammatory activation profile
179 consistent with previous studies.

180 To confirm that HIV-1 JRFL infection of human iPSC-derived microglia resulted in
181 productive infection and inflammatory activation, we chose a female iPSC line, CD06, and
182 infected it with the JRFL strain as well as a second R5 tropic HIV-1 strain, YU2 (Li et al. 1991),
183 isolated from the CSF of a different patient with severe HAND. We confirmed infection by RT–
184 qPCR of viral *gag-pol* RNA, which exhibited significantly increased expression for both strains by
185 day 16 post-infection, with a subsequent decrease (**Figure 3A**). Using ELISA to detect secreted
186 p24 revealed productive infection for both viral strains (**Figure 3B**). We then assessed the

187 expression of key inflammatory markers and microglial core mRNAs by qPCR. Both JRFL and
188 YU2 infections led to a significant increase in IL1β expression compared to uninfected microglia
189 (**Figure 3C**). Similarly, TNFα was significantly upregulated in the first two weeks of infection but
190 decreased as the productive infection waned (**Figure 3C**). We also observed increased
191 expression of the chemokines CCL2 and CCL3 by days 16 and 23 post infection with both strains
192 (**Figure 3D**). This upregulation then decreased by day 27, correlating with the reduction of
193 productive infection as indicated by the p24 ELISA (**Figure 3A**). In comparison to the unaltered
194 IBA1 expression we found previously, HIV-1 led to a significant reduction in IBA1 expression in
195 CD06 infected microglia (**Figure 3E**). Similar to 03SF infected microglia, CD06 had significant
196 increased expression of P2RY12 (**Figure 3E**). Together, these results demonstrate infectability
197 of human iPSC-derived microglia with multiple, macrophage tropic HIV-1 strains and their ability
198 to elicit an inflammatory response.
199

200 **Type I interferon stimulated gene expression and sustained activation following HIV-1**
201 **infection**

202 To investigate the transcriptional landscape of HIV-1 infected microglia, we performed bulk RNA
203 sequencing on male 03SF iPSC-derived microglia infected by HIV-1 JRFL day 16 post infection.
204 Principal component analysis (PCA) revealed clear separation of the infected vs mock infected
205 samples (**Figure S2**). Differential gene analysis revealed differentially expressed genes (DEGs)
206 including several classic ISGs, such as IFIT3, MX2, ISG15, RSAD2 and others (**Figure 4A**) (**Table**
207 **S2**). Gene set enrichment analysis (GSEA) confirmed a significant enrichment of genes related
208 to the interferon alpha response (**Table S3**) (**Figure 4B**). Gene ontology analysis identified
209 activation of innate immune responses and several related terms in the biological process
210 component (**Figure 4C, D** and **Figure S3**). The upregulated DEG GO set includes pathways
211 falling into the overall signaling clusters related to interferon signaling and positive regulation of
212 antiviral biotic, interferon alpha/beta, defense against virus, cytokine mediated and interferon

213 mediated pathways, and negative regulation of viral processes. Among the downregulated DEG
214 GO clusters are pathways related to positive regulation of antigen processing, extracellular
215 organization, granulocyte/leukocyte migration, chemokine-mediated signaling, and spindle
216 assembly checkpoints. Importantly, HIV-1 infection was found to lead to significant induction of
217 many ISGs, including ISG15, IRF7, MX1, OAS1, OAS2, OAS3, STAT1, CXCL10, and IFITM3
218 (**Figure 4A, E**). **Figure 4F** shows the expression of various genes encoding SIGLEC proteins that
219 are responsible for regulating microglial cell–cell interactions [Reviewed in (Crocker, Paulson, and
220 Varki 2007)]. Consistent with previous studies, we found that HIV-1 infection causes significant
221 upregulation of SIGLEC1, which has been implicated in the direct cell–cell transmission of HIV
222 (Izquierdo-Useros et al. 2012; Zou et al. 2011). However, we found that SIGLEC11 and
223 SIGLEC16 were significantly downregulated after infection.

224 We then validated the expression of a subset of the ISGs identified in the sequencing
225 dataset by RT–qPCR of JRFL infected 03SF iPSC-derived microglia. We found significant
226 upregulation of CXCL10, RSAD2, ISG15, and IDO1 (**Figure 4G**). Elevated expression of these
227 genes persisted over an additional week of infection on day 23 (**Figure 4G**). Additionally, we
228 performed RT–qPCR on CD06 iPSC-derived microglia infected with either JRFL or YU2 HIV
229 strains. We also found increased expression of CXCL10 and RSAD2 in these HIV-infected cells;
230 however, only the day 16 YU2 condition reached significance (**Figure 4H**). Comparison of Figure
231 4G and 4H indicates potential differences with infecting different cell lines. Together, these data
232 support the conclusion that HIV-1 infection induces sustained type I interferon signaling in iPSC-
233 derived microglia and alters the gene regulation of many microglial biological processes including
234 interferon signaling.

235

236 **HIV-1 infected microglia incorporate into cerebral organoids**

237 After characterizing the response of isolated human iPSC-derived microglia to HIV-1 infection we
238 then investigated whether HIV-1 infected microglia could incorporate into iPSC-derived cerebral

239 organoids and whether interferon signaling was similarly upregulated in microglia and potentially
240 other neural cell types. Cerebral organoids were grown using modified, published protocols
241 (Lancaster and Knoblich 2014; Paşca et al. 2015; Sloan et al. 2018; Yoon et al. 2019; Qian et al.
242 2020; Xu et al. 2021). To create microglia-containing organoids, we cocultured human microglia
243 with sliced neocortical organoids (SNO), prepared as described previously (Qian et al. 2020).
244 SNOs exhibit enhanced neurogenesis and laminar expansion (Qian et al. 2020). We found that
245 microglia exhibit the ability to incorporate with organoid slices to form human microglia containing
246 sliced neocortical organoids (mSNOs). **Figure 5A** shows mSNO containing neurons ($MAP2^+$),
247 astrocytes ($GFAP^+$), and microglia ($IBA1^+$). These neuroimmune organoids provide a model
248 system for studying the impact of HIV-1 infection on the physiology, localization, and interactions
249 of these three cell types.

250 To create an HIV-1 infected human cerebral organoid, we infected 03SF iPSC-derived
251 microglia with JRFL HIV. Following 2 weeks in culture, infected or noninfected microglia were
252 added to 400 μM organoid slices and cultured for 2 additional weeks. On day 14 post coculture
253 with microglia, mSNOs were fixed for immunohistochemistry or total RNA was extracted for RT–
254 qPCR analysis. HIV-1-infected microglia ($p24^+$, $IBA1^+$) were detected in a mSNO (**Figure 5B&C**).
255 Interestingly, neurons ($MAP2^+$) appeared to be sparser in regions of HIV-1-infected microglia
256 (**Figure 5B** "arrows"). These regions had scattered $MAP2^+$ processes (**Figure 5B1**) compared
257 with the denser MAP2 staining throughout the bulk of the organoid. HIV-1 *gag/pol* RNA exhibited
258 significant expression in mSNOs containing HIV-1 infected microglia (**Figure 5D**). To provide
259 evidence of productive infection in mSNOs, we identified secreted p24 only in the media of
260 organoid cultures that had received HIV-1 infected microglia (**Figure 5E**).

261 Because we observed significant and sustained interferon signaling in microglial
262 monocultures, we evaluated mRNA expression of a panel of ISGs (ISG15, RSAD2, IFITM3, MX1,
263 IFI44, IFI27). We found that ISG15 mRNA was significantly upregulated and RSAD2 also showed
264 an increasing trend of expression in mSNOs containing HIV-1 infected microglia (**Figure 5F**).

265 IFITM3 has been touted as a marker for interferon-responsive microglia and has been shown to
266 play a newly discovered role in amyloid precursor protein processing to amyloid beta (Hur et al.
267 2020). Interestingly, we found significant upregulation of IFITM3 mRNA in mSNOs containing
268 HIV-1 infected microglia (**Figure 5F).** We also evaluated the expression of MX1, IFI27, and IFI44,
269 which, along with ISG15 and RSAD2, were among the top 10 persistently upregulated genes in
270 a recent study on two cohorts of 22 HIV-1 seroconverts from Uganda and 22 from South Africa
271 (Mackelprang et al. 2023). Expression of MX1, IFI27, and IFI44 appeared to be increased but
272 failed to reach significance. Especially considering the small fraction of HIV-1 infected microglia
273 in the cultured mSNO (**Figure 5B**), these increases suggest that HIV-1 infected microglia are
274 associated with increased interferon signaling in the organoids and may have indirect
275 consequences for neuronal viability and inflammatory responses in other cell types.
276
277 **DISCUSSION:**
278 In this study, we used iPSC-derived human microglia and microglia containing cortical organoids
279 to model HIV-1 related neuroimmune dysregulation and pathology. In this model, iPSC-derived
280 microglia were shown to be infected with two strains of replication competent HIV-1, JRFL and
281 YU2, and exhibited inflammatory activation, as shown by gene expression changes and
282 cytokine/chemokine secretion (**Figures 2 & 3**). Importantly, we found persistent activation of type
283 I interferon response pathways and downstream interferon stimulated genes (ISGs), which may
284 have important implications for understanding the pathogenesis of HAND.
285 In comparison to the recently developed primary human neural progenitor cell-derived
286 organoid HIV-1 model (dos Reis et al. 2020) and the 2D neuron, astrocyte, and microglia
287 "triculture" HIV-1 model (Ryan et al. 2020), an iPSC-derived human microglia containing sliced
288 neocortical organoid model has distinct advantages. Organoids recapitulate 3D cell-cell and cell-
289 matrix interactions more faithfully than 2D cultures and develop complex tissue architecture
290 (Lancaster et al. 2013; Paşca et al. 2015; Birey et al. 2017; Quadrato et al. 2017; Velasco et al.

291 2019); thus, organoids are well suited to studying aspects of altered brain anatomy and physiology
292 seen in individuals with *HAND* (Di Sclafani et al. 1997; Clifford et al. 2017; Israel et al. 2019).
293 While others have also generated microglia containing organoids using a protocol in which
294 microglia innately develop within organoids, this system is associated with a high degree of
295 heterogeneous cell types (Gumbs et al. 2022), which could make dissection of the relative
296 contributions and effects on specific cell types more complex. In our method, we have greater
297 freedom to manipulate the timing, proportion, and infection stage of microglia addition in sliced
298 neocortical organoids. While some previous studies used pseudotyped virus (dos Reis et al.
299 2020), our study examined infection using two macrophage tropic, replication competent strains
300 of HIV-1. Our findings, showing induction of inflammatory gene expression associated with active
301 viral expression align with recent studies on brain samples from HIV-1^{+} patients from the National
302 NeuroAIDS Tissue Consortium (NNTC). In that study, HIV-1 RNA load was found to correlate with
303 increased interferon signaling and inflammatory gene sets while inversely correlating with
304 neuronal and synaptic gene sets, suggesting neuronal pathology (Sanna et al. 2021).

305 Microglia secrete diverse cytokines and chemokines implicated in HIV-1 neuropathology
306 (Hanisch 2002; Ramesh, MacLean, and Philipp 2013; Chen et al. 2017). Cytokine/chemokine
307 analysis of the supernatant of HIV-1 infected microglia identified the secretion of M-CSF and IP-
308 10/CXCL10 (**Figure 2F**). M-CSF overexpression has been linked to microglial proliferation,
309 increased phagocytosis, cytokine secretion, and inflammatory responses in both Alzheimer's
310 disease (AD) and HAND, as well as increased microglial susceptibility to HIV-1 infection and
311 increased virus replication (Gallo et al. 1990; Kalter et al. 1991; Kutza et al. 2000; Mitrasinovic et
312 al. 2001; Kutza et al. 2002; Smith et al. 2013). IP-10/CXCL10 is a chemotactic chemokine that
313 recruits leukocytes, T cells, and monocytes while also being neurotoxic and strongly correlated
314 with HIV-1 related disease progression (van Marle et al. 2004; Jiao et al. 2012; Lei et al. 2019).
315 Clinical studies have shown elevated IP-10/CXCL10 levels (~200-1000 pg/ml) in the cerebral
316 spinal fluid of HIV-1^{+} individuals (Kolb et al. 1999; Peluso et al. 2017); these levels are strikingly

317 similar to our observations (**Figure 2F**). CXCL10/IP-10 has been shown to be induced by HIV-1
318 proteins gp120, Nef, and Tat (Kutsch et al. 2000; Asensio et al. 2001; van Marle et al. 2004; Lei
319 et al. 2019). Importantly, IP-10/CXCL10 and RANTES (CCL5) were the strongest predictors of
320 neurocognitive impairment in a screen of 139 HIV-1^{+} individuals (Ruhanya et al. 2021), similar to
321 findings from earlier studies (Valverde-Villegas et al. 2018; Burlacu et al. 2020). HIV-1 brain
322 infection leads to an abnormal inflammatory state and dysregulated cytokine/chemokine
323 production (Kaul, Garden, and Lipton 2001; González-Scarano and Martín-García 2005; Burdo,
324 Lackner, and Williams 2013). Despite this knowledge, there remains a large gap in our
325 understanding of how CXCL10 and other cytokines/chemokines associated with CNS HIV-1
326 infection alter aspects of neuronal excitability, synaptic transmission, and inward and outward
327 currents vital to healthy neuronal physiology.

328 A striking finding in our study was the persistent activation of interferon response genes.
329 Induction of these pathways is known to be a hallmark of HIV-1 infection in monocytes and
330 macrophages, much more prominently than in T cells (Berg et al. 2014; Aso et al. 2019; Elsner et
331 al. 2020; Jeremiah et al. 2023). Thus, it is not surprising to have seen this strong response in
332 microglia, which share many physiologic properties with macrophages [reviewed in (Li and Barres
333 2018)]. Most studies suggest that the interferon response is relatively transient; thus, the
334 persistent expression of at least a subset of ISGs may be a relatively unique feature of microglial
335 HIV-1 infection that may have important pathophysiologic consequences. Increasing evidence
336 suggests a role for type I interferons in cognitive-related deficits seen in patients with various
337 neurodegenerative diseases. Using single-cell sequencing, researchers have dissected a unique
338 sub-population of interferon-responsive microglia that may potentiate dysregulated immune
339 interactions in the form of aberrant pruning of synapses, altered phagocytic function, and
340 dysregulated cytokine/chemokine production (Jin et al. 2022). Constitutive overexpression of type
341 I interferons seen in the “interferonopathies” can be associated with profound CNS disease
342 [reviewed in (Goldmann, Blank, and Prinz 2016), and (Blank and Prinz 2017)](Wiley, Steinman,

343 and Wang 2023). Patients receiving type I interferons therapeutically may experience cognitive
344 impairment and neurological symptoms (Christina, Randall, and Arthur 1991; Pavol et al. 1995;
345 Capuron, Ravaud, and Dantzer 2001; Capuron et al. 2002; Wichers et al. 2005; Raison et al.
346 2005).

347 Whether interferon induction inhibits or enhances HIV infection and latency in microglia
348 remains to be understood. Recent studies have highlighted that interferon can inhibit HIV infection
349 of primary microglia but less so of iPSC-derived microglia, as well as macrophages (Nasr et al.
350 2017; Woodburn et al. 2022). Interestingly, interferon may promote latency in macrophages
351 (Dickey et al. 2022). An important feature of HIV infection of microglia identified in previous in vitro
352 studies has been the rapid induction of viral latency (Alvarez-Carbonell et al. 2019; Sreeram et
353 al. 2022). Our cerebral organoid model will provide an interesting system to examine the induction
354 of HIV latency, its reactivation, and its effects on both adjacent and more distant neural cells.

355 An important future direction, facilitated by the development of this model system, will be
356 experiments aimed at understanding the functional consequences that HIV infection,
357 dysregulated interferon signaling, inflammatory activity, and changes in other important genes
358 expressed in the CNS, may have on neuronal synaptic transmission. A number of ISGs have
359 predicted downstream effects that could trigger or enhance neurodegeneration. For example,
360 indoleamine 2,3-dioxygenase 1 (IDO) is a key enzyme in tryptophan catabolism, leading to the
361 formation of kynurenic acid, an antagonist of NMDA receptors (Schwarcz and Stone 2017). This
362 pathway and its products, such as the neurotoxin and NMDAR antagonist quinolinic acid, have
363 been previously implicated in neurodegenerative diseases, including Huntington's, Alzheimer's
364 and Parkinson's disease (Malpass 2011; Maddison and Giorgini 2015).

365 Overall, the HIV-1 mSNO model presents an effective in vitro platform for investigating the
366 underlying molecular and cellular mechanisms associated with HIV-1 and human neural cell
367 interactions. **Our results predict that interferon stimulated genes likely play a role in altering**
368 **neuronal function and contributing to HAND.**

ACKNOWLEDGEMENTS

This work was supported in part by grants from the NIH (R21NS120806), a Rutgers Busch Biomedical Grant, a Rutgers Brain Health Institute Pilot Grant, and the Robert Wood Johnson Foundation (Grant #74260). AJB was supported by NIH NIGMS T32GM8339 and NIH NCATS TL1TR003019.

AUTHOR CONTRIBUTIONS

AJB, ZPP, PJ, RPH, and ABR conceived the study. AJB designed the experiments and interpreted the data. AJB performed most of the experiments with technical assistance from ACS, HL, and YA. ACS and AJB performed qPCR. HL and AJB performed ELISA. AJB performed immunocytochemistry, immunohistochemistry, and confocal imaging. AJB and HS performed viral infections. RPH and AJB performed computational analysis of RNA-seq data. AJB prepared the figures and wrote the manuscript with input from all coauthors.

COMPETING FINANCIAL INTERESTS

The authors declare no competing financial interests.

387 **METHODS**

388

389 **Human induced pluripotent stem cell maintenance**

390 Three human iPSC lines were used in this study (male 03SF iPSC line; female CD06 iPSC line;
391 male CD52 iPSC line). Human iPSCs were cultured in stem cell medium consisting of MACs iPS-
392 Brew XF complete media. The culture medium was changed daily. Human iPSCs were passaged
393 one to two times per week onto new plates coated with Matrigel. Human iPSCs were detached
394 with Accutase treatment for 5 min and centrifuged at 120 rcf for 5 min. The pellet was resuspended
395 in stem cell medium plus Y-27632 (10 μM). The iPSCs used in this study were below passage
396 50. All studies were performed with protocols approved by Rutgers University.

397

398 **Generation of microglia**

399 Primitive microglia precursors (PMPs) were generated from 3 iPSC cell lines using a previously
400 established protocol (Haenseler et al. 2017). iPSCs were detached with Accutase, plated at
401 20,000 cells per well in a 96-well low-adherence plate in yolk sac induction medium plus the rock
402 inhibitor Y-27632 (10 μM), and centrifuged at 1000 rpm for 3 min to aggregate the cells for
403 embryoid body formation. Yolk-sac induction medium consisted of MAC iPS-Brew XF complete
404 media plus bone morphogenetic protein 4 (BMP4, 50 ng/ml), vascular endothelial growth factor
405 (VEGF, 50 ng/ml), stem cell factor (SCF, 20 ng/ml), and ß-mercaptoethanol. Yolk-sac induction
406 media was given for the first 5 days of culture. On day 6, YS-EBs were plated in 100 mm cell
407 culture plates in factory media consisting of XVIVO15 supplemented with 0.5% NEAA, ß-
408 mercaptoethanol, macrophage colony stimulating factor (M-CSF, 100 ng/ml) and interleukin-3 (25
409 ng/ml). At 2-4 weeks after plating, human PMPs egress from the yolk sac lumen into the
410 surrounding media and are continuously produced for more than 3 months.

411 To mature PMPs into microglia, PMPs were transitioned to maturation media composed
412 of XVIVO15 supplemented with N2, Glutamax, 0.5% NEAA, interleukin-34 (IL-34, 100 ng/ml),

413 granulocyte macrophage colony stimulating factor (GM-CSF, 10 ng/ml, and M-CSF (25 ng/ml) for
414 1-2 weeks. The medium was changed every 4 days. Cells were then detached with 20 min
415 Accutase treatment and used for experiments.
416
417 **Generation of iPSC-derived Cerebral Organoids**
418 Cerebral organoids were generated from 1 iPSC line using adapted previously published
419 protocols (Qian et al. 2020). In this study, 9,000 iPSCs were cultured in low-adherence 96-well
420 plates to form uniform embryoid bodies. On day 1, the medium was changed to neural induction
421 medium composed of DMEM/F12 supplemented with 1X N2, 2 μM A83-01, and 2 μM
422 dorsomorphin. On days 5 and 6, half of the medium was replaced with DMEM/F12 supplemented
423 with 1X N2, 10 μM SB431542, and 1 μM CHIR99021. On day 7, EBs were embedded in a Growth-
424 Factor-Reduced Matrigel 'cookie' as previously described (Qian et al. 2020). Half of the medium
425 was changed every two days until day 14. On day 14, organoids were dissociated from the
426 Matrigel cookie and placed in low-adherence 6-well plates on an orbital shaker at 85 rpm. On day
427 16, organoids were fed 1:1 DMEF12: Neurobasal, 1X N2, 1X B27-RA, 0.5% NEAA, and 200 μM
428 L-AA. Media was replenished every 2-3 days until day 30. On day 30, the medium was changed
429 to 1:1 DMEF12: Neurobasal, 1X N2, 1X B27, 0.5% NEAA, 200 μM L-AA, and.25% GFR-Matrigel.
430 Half of the media was changed every 3-4 days.
431
432 **Organoid Slicing**
433 To create sliced neocortical organoid cultures, cerebral organoids were sectioned with a
434 vibratome and transferred back into in vitro cell culture. Briefly, a fresh stock of 3% low-melting
435 temperature agarose in PBS was prepared and kept at 39°C to remain liquid. Artificial cerebral
436 spinal fluid (ACSF) for sectioning contained (in mM): NaCl 125, KCl 2.5, $NaH_2PO_4 \cdot H_2O$ 1.25,
437 $NaHCO_3$ 25, $MgCl_2$ 1.2, $CaCl_2$ 2.5, glucose ($C_6H_{12}O_6$) 2.5, and sucrose ($C_{12}H_{22}O_{11}$) 22.5. The
438 ACSF was then bubbled with 5% CO_2/95% O_2 for 10 minutes before bivalent cations (in mM):

439 $MgCl_2$ 1.2, $CaCl_2$ 0.625. The solution was then filtered through a 0.2-micron PES filter and returned
440 to bubbling on ice. Cerebral organoids were then transferred to 37°C DMEF12, 200 μM L-AA, and
441 55 μM beta-mercaptoethanol before being embedded in 3% low-melting temperature agarose.
442 The agarose block containing organoids was then sectioned at 400 μM thickness. Slices were
443 then subjected to two washing processes in Primocin-treated media to reduce the chance of
444 contamination.
445
446 **HIV-1 Stock Preparation**
447 HIV-1 JRFL virus (ARP-395) and HIV-1 YU2 proviral DNA (ARP-1350) were obtained through
448 the NIH HIV Reagent Program, Division of AIDS, NIAID. HIV-1 JRFL was propagated in
449 phytohemagglutinin (PHA, 5 μg/ml)-stimulated human peripheral blood mononuclear cells.
450 Viruses were harvested on days 7-10 post infection. HIV-1 YU2 stocks were generated by
451 transfection of 293T cells with HIV-1 YU2 proviral DNA. The transfected cells were cocultivated
452 with PHA-PBMCs 48 h after transfection, and cell supernatants were harvested 7 days after
453 coculture. The YU2 HIV stocks were further propagated in PHA-PBMCs as described. The
454 amount of viral p24 was determined using the HIV-1 Gag p24 DuoSet ELISA (R &D System,
455 DY7360-05).
456
457 **HIV-1 infection**
458 PMPs were matured for 1-2 weeks in microglia maturation medium. Matured PMPs were then
459 incubated with 2 ng/ml p24 of either JRFL strain or YU2 strain HIV-1 (NIH AIDS Repository) for
460 24 hours at 300,000 cells per 100 μl of media. After 24 hours, DMEF12 was added, and the cells
461 were centrifuged for 3 min at 120 rcf. The cells were then resuspended in microglia maturation
462 media minus M-CSF and plated. Half of the media was changed every 3-6 days.
463
464 **HIV-1 2-LTR circles PCR**

465 For detection of HIV 2LTR circles, total DNA (including small nongenomic DNA) was isolated
466 with a DNeasy Blood and Tissue kit (Qiagen 69504). End point PCR analysis (Taq 2X Master
467 Mix, NEB) was performed using 300 ng DNA template and 2-LTR circle primers: forward,
468 MH535: 5′-AACTAGGGAACCCACTGCTTAAG-3′; reverse, MH536: 5′-
469 TCCACAGATCAAGGATATCTTGTC-3′ (Butler, Hansen, and Bushman 2001).
470
471 **Tissue preparation**
472 Organoids were fixed in 4% PFA overnight at 4°C. Organoids were then transferred to 15%
473 sucrose and 0.05% sodium azide in PBS for 24 hours, followed by another 24 hours in 30%
474 sucrose and 0.05% sodium azide in PBS. Organoids were then embedded in OCT freezing
475 medium and snap frozen on an ethanol dry ice slurry. Frozen embedded organoids were given at
476 least 3 hours to warm to -20°C before cryosectioning on a Leica cryostat at thicknesses between
477 10-30 μM. Sections were mounted on charged microscope slides (VWR) and placed on a slide
478 warmer at 37°C for 30 min. Slides were then stored in a slide box at -20°C until used for staining.
479
480 **Immunofluorescence**
481 For immunocytochemistry, half of the medium was left in each well with an equal amount of 4%
482 PFA and then added at a final concentration of 2% PFA overnight at 4°C. The next day, PFA was
483 removed, and the cells were washed with PBS plus 0.3 M glycine for 30 min. The cells were then
484 permeabilized with 0.2% Triton X-100 in PBS for 7 min. The cells were then blocked for 1 hour in
485 blocking buffer consisting of 5% normal goat serum (NGS), 4% bovine serum albumin (BSA),
486 0.05% Triton X-100, 0.05% sodium azide, and PBS.
487 For immunohistochemistry, cryosectioned organoid slides were warmed to 37°C for 5 min.
488 A hydrophobic barrier was then drawn around the specimens and allowed to dry for 5 min. PBS
489 plus 0.3 M glycine was then added in a liquid dome over the specimens to rehydrate for 10 min.
490 Sections were permeabilized with 0.5% Triton X-100, 0.3 M glycine, and PBS for 1 hr. After

491 permeabilization, the sections were blocked with blocking solution consisting of 5% normal goat
492 serum, 4% BSA, 0.05% Triton X-100, 0.05% sodium azide, and PBS for 1 hr. Primary antibodies
493 were diluted in blocking solution and applied to the sections overnight at 4°C. The primary
494 antibodies and their dilutions are summarized in the Key Resources Table. After washing with
495 0.05% Triton X-100 and PBS (PBST) 5 times, secondary antibodies diluted in blocking buffer
496 were added for 1 hr at RT. Finally, the sections were washed five times with PBST before a final
497 wash in deionized water and mounting with DAPI Fluoroshield (Fisher). Secondary antibodies
498 were Alexa Fluor 488-, 546-, 633- or 647-conjugated goat antibodies (Invitrogen) used at a 1:500
499 dilution. Images were taken on a Zeiss LSM700 confocal microscope.
500
501 **RNA isolation**
502 Total RNA was prepared with an RNeasy Plus kit (Qiagen) with preprocessing through
503 Qiashredder (Qiagen) and frozen at -80°C.
504
505 **RT–qPCR**
506 cDNA was generated using SuperScript VILO Master mix. RNA expression was measured using
507 SYBR green on a QuantStudio 3 (Agilent). Probes were generated using NCBI primer blast and
508 are listed in Table X. Two technical replicates were performed per sample. When a high standard
509 deviation between replicates occurred, replicates were rerun in triplicate. All expression levels
510 were normalized to GAPDH expression and represented as $2^{-(\Delta\Delta CT)}$. For null result values where
511 a ct was not achieved, a max ct value of 40 was used for statistical analysis.
512
513 **Bulk RNA sequencing and analysis**
514 We performed bulk RNA-sequencing analysis of iPSC-derived microglia. Total RNA was prepared
515 using an RNeasy kit (QIAGEN). Library construction and sequencing were performed by
516 Novogene. The libraries were subjected to 75 bp paired read sequencing using a NextSeq500

517 Illumina sequencer. Approximately 30–36 million paired reads were generated for each sample.
518 Bc12Fastq software, version 1.8.4, was used to generate Fastq files. The genome sequence was
519 then indexed using the rsem-prepare-reference command.
520 Each fastq file was trimmed and checked for quality with fastp (v. 0.12.2) and then aligned
521 to the UCSC hg38 human genome using HISAT2 (v.2.1.0)71,72. Transcript counts were extracted
522 using the featureCounts function of the Rsubread package.
523
524 **Statistics and reproducibility.** All data represent the mean ± s.e.m. When only two independent
525 groups were compared, significance was determined by a two-tailed unpaired t test with Welch's
526 correction. A p value <0.05 was considered significant. The analyses were performed in
527 GraphPad Prism v.9. All experiments were independently performed at least three times with
528 similar results.

References:

Abud, Edsel M., Ricardo N. Ramirez, Eric S. Martinez, Luke M. Healy, Cecilia H. H. Nguyen, Sean A. Newman, Andriy V. Yeromin, Vanessa M. Scarfone, Samuel E. Marsh, Cristhian Fimbres, Chad A. Caraway, Gianna M. Fote, Abdullah M. Madany, Anshu Agrawal, Rakez Kayed, Karen H. Gylys, Michael D. Cahalan, Brian J. Cummings, Jack P. Antel, Ali Mortazavi, Monica J. Carson, Wayne W. Poon, and Mathew Blurton-Jones. 2017. 'iPSC-Derived Human Microglia-like Cells to Study Neurological Diseases', *Neuron*, 94: 278-93.e9.

Alvarez-Carbonell, D., F. Ye, N. Ramanath, Y. Garcia-Mesa, P. E. Knapp, K. F. Hauser, and J. Karn. 2019. 'Cross-talk between microglia and neurons regulates HIV latency', *PLoS Pathog*, 15: e1008249.

Alvarez-Carbonell, David, Fengchun Ye, Nirmala Ramanath, Yoelvis Garcia-Mesa, Pamela E. Knapp, Kurt F. Hauser, and Jonathan Karn. 2020. 'Cross-talk between microglia and neurons regulates HIV latency', *PLOS Pathogens*, 15: e1008249.

Anderson, Albert M., Jeffrey L. Lennox, Mark M. Mulligan, David W. Loring, Henrik Zetterberg, Kaj Blennow, Cari Kessing, Rajeth Koneru, Kirk Easley, and William R. Tyor. 2017. 'Cerebrospinal fluid interferon alpha levels correlate with neurocognitive impairment in ambulatory HIV-Infected individuals', *Journal of NeuroVirology*, 23: 106-12.

Asensio, V. C., J. Maier, R. Milner, K. Boztug, C. Kincaid, M. Moulard, C. Phillipson, K. Lindsley, T. Krucker, H. S. Fox, and I. L. Campbell. 2001. 'Interferon-independent, human immunodeficiency virus type 1 gp120-mediated induction of CXCL10/IP-10 gene expression by astrocytes in vivo and in vitro', *Journal of Virology*, 75: 7067-77.

Aso, H., J. Ito, Y. Koyanagi, and K. Sato. 2019. 'Comparative Description of the Expression Profile of Interferon-Stimulated Genes in Multiple Cell Lineages Targeted by HIV-1 Infection', *Front Microbiol*, 10: 429.

Baruch, Kuti, Aleksandra Deczkowska, Eyal David, Joseph M. Castellano, Omer Miller, Alexander Kertser, Tamara Berkutzki, Zohar Barnett-Itzhaki, Dana Bezalel, Tony Wyss-Coray, Ido Amit, and Michal Schwartz. 2014. 'Aging-induced type I interferon response at the choroid plexus negatively affects brain function', *Science*, 346: 89-93.

Berg, R. K., S. H. Rahbek, E. Kofod-Olsen, C. K. Holm, J. Melchjorsen, D. G. Jensen, A. L. Hansen, L. B. Jørgensen, L. Ostergaard, M. Tolstrup, C. S. Larsen, S. R. Paludan, M. R. Jakobsen, and T. H. Mogensen. 2014. 'T cells detect intracellular DNA but fail to induce type I IFN responses: implications for restriction of HIV replication', *PLoS One*, 9: e84513.

Birey, Fikri, Jimena Andersen, Christopher D. Makinson, Saiful Islam, Wu Wei, Nina Huber, H. Christina Fan, Kimberly R. Cordes Metzler, Georgia Panagiotakos, Nicholas Thom, Nancy A. O'Rourke, Lars M. Steinmetz, Jonathan A. Bernstein, Joachim Hallmayer, John R. Huguenard, and Sergiu P. Paşca. 2017. 'Assembly of functionally integrated human forebrain spheroids', *Nature*, 545: 54-59.

Blank, T., and M. Prinz. 2017. 'Type I interferon pathway in CNS homeostasis and neurological disorders', *Glia*, 65: 1397-406.

Burdo, Tricia H., Andrew Lackner, and Kenneth C. Williams. 2013. 'Monocyte/macrophages and their role in HIV neuropathogenesis', *Immunological Reviews*, 254: 102-13.

Burlacu, R., A. Umlauf, T. D. Marcotte, B. Soontornniyomkij, C. C. Diaconu, A. Bulacu-Talnariu, A. Temereanca, S. M. Ruta, S. Letendre, L. Ene, and C. L. Achim. 2020. 'Plasma CXCL10 correlates with HAND in HIV-infected women', *Journal of NeuroVirology*, 26: 23-31.

44 Butler, S. L., M. S. Hansen, and F. D. Bushman. 2001. 'A quantitative assay for HIV DNA integration in
45 vivo', *Nat Med*, 7: 631-4.
46 Byrnes, S. J., T. A. Angelovich, K. Busman-Sahay, C. R. Cochrane, M. Roche, J. D. Estes, and M. J.
47 Churchill. 2022. 'Non-Human Primate Models of HIV Brain Infection and Cognitive Disorders',
48 *Viruses*, 14.
49 Capuron, Lucile, Jane F. Gumnick, Dominique L. Musselman, David H. Lawson, Andrea Reemsnyder,
50 Charles B. Nemeroff, and Andrew H. Miller. 2002. 'Neurobehavioral Effects of Interferon-α in
51 Cancer Patients: Phenomenology and Paroxetine Responsiveness of Symptom Dimensions',
52 *Neuropsychopharmacology*, 26: 643-52.
53 Capuron, Lucile, Alain Ravaud, and Robert Dantzer. 2001. 'Timing and Specificity of the Cognitive
54 Changes Induced by Interleukin-2 and Interferon-α Treatments in Cancer Patients',
55 *Psychosomatic Medicine*, 63.
56 Casano, Alessandra Maria, and Francesca Peri. 2015. 'Microglia: Multitasking Specialists of the Brain',
57 *Developmental Cell*, 32: 469-77.
58 Chargelegue, Daniel, and Carol M. O'Toole. 1992. 'Development of a sensitive ELISA for HIV-1 p24
59 antigen using a fluorogenic substrate for monitoring HIV-1 replication in vitro', *Journal of*
60 *Virological Methods*, 38: 323-32.
61 Chen, Natalie C., Andrea T. Partridge, Christian Sell, Claudio Torres, and Julio Martín-García. 2017. 'Fate
62 of microglia during HIV-1 infection: From activation to senescence?', *Glia*, 65: 431-46.
63 Christina, A. Meyers, S. Scheibel Randall, and D. Forman Arthur. 1991. 'Persistent neurotoxicity of
64 systemically administered interferon-alpha', *Neurology*, 41: 672.
65 Claes, Christel, Johanna Van den Daele, and Catherine M. Verfaillie. 2018. 'Generating tissue-resident
66 macrophages from pluripotent stem cells: Lessons learned from microglia', *Cellular*
67 *Immunology*, 330: 60-67.
68 Clifford, Katherine M., Vishal Samboju, Yann Cobigo, Benedetta Milanini, Gabriel A. Marx, Joanna M.
69 Hellmuth, Howard J. Rosen, Joel H. Kramer, Isabel E. Allen, and Victor G. Valcour. 2017.
70 'Progressive Brain Atrophy Despite Persistent Viral Suppression in HIV Patients Older Than 60
71 Years', *Journal of acquired immune deficiency syndromes (1999)*, 76: 289-97.
72 Crocker, Paul R., James C. Paulson, and Ajit Varki. 2007. 'Siglecs and their roles in the immune system',
73 *Nature Reviews Immunology*, 7: 255-66.
74 Di Sclafani, V., R. D. Mackay, D. J. Meyerhoff, D. Norman, M. W. Weiner, and G. Fein. 1997. 'Brain
75 atrophy in HIV infection is more strongly associated with CDC clinical stage than with cognitive
76 impairment', *Journal of the International Neuropsychological Society : JINS*, 3: 276-87.
77 Dickey, L. L., L. J. Martins, V. Planelles, and T. M. Hanley. 2022. 'HIV-1-induced type I IFNs promote viral
78 latency in macrophages', *J Leukoc Biol*, 112: 1343-56.
79 dos Reis, Roberta S., Shilpa Sant, Hannah Keeney, Marc C. E. Wagner, and Velpandi Ayyavoo. 2020.
80 'Modeling HIV-1 neuropathogenesis using three-dimensional human brain organoids (hBORGs)
81 with HIV-1 infected microglia', *Scientific Reports*, 10: 15209.
82 Durafourt, B. A., C. S. Moore, D. A. Zammit, T. A. Johnson, F. Zaguia, M. C. Guiot, A. Bar-Or, and J. P.
83 Antel. 2012. 'Comparison of polarization properties of human adult microglia and blood-derived
84 macrophages', *Glia*, 60: 717-27.
85 Eggers, C., G. Arendt, K. Hahn, I. W. Husstedt, M. Maschke, E. Neuen-Jacob, M. Obermann, T.
86 Rosenkranz, E. Schielke, and E. Straube. 2017. 'HIV-1-associated neurocognitive disorder:
87 epidemiology, pathogenesis, diagnosis, and treatment', *J Neurol*, 264: 1715-27.

88 Elsner, C., A. Ponnurangam, J. Kazmierski, T. Zillinger, J. Jansen, D. Todt, K. Döhner, S. Xu, A. Ducroux,
89 N. Kriedemann, A. Malassa, P. K. Larsen, G. Hartmann, W. Barchet, E. Steinmann, U. Kalinke, B.
90 Sodeik, and C. Goffinet. 2020. 'Absence of cGAS-mediated type I IFN responses in HIV-1-
91 infected T cells', *Proc Natl Acad Sci U S A*, 117: 19475-86.
92 Eugenin, E. A., and J. W. Berman. 2016. 'Improved Methods to Detect Low Levels of HIV Using
93 Antibody-Based Technologies', *Methods Mol Biol*, 1354: 265-79.
94 Gallo, Paolo, Silvana Pagni, Bruno Giometto, Maria G. Piccinno, Felice Bozza, Vincenza Argentiero, and
95 Bruno Tavolato. 1990. 'Macrophage-colony stimulating factor (M-CSF) in the cerebrospinal
96 fluid', *Journal of Neuroimmunology*, 29: 105-12.
97 Gendelman, Howard E., Stuart A. Lipton, Marc Tardieu, Michael I. Bukrinsky, and Hans S. L. M. Nottet.
98 1994. 'The neuropathogenesis of HIV-1 infection', *Journal of Leukocyte Biology*, 56: 389-98.
99 Goldmann, T., T. Blank, and M. Prinz. 2016. 'Fine-tuning of type I IFN-signaling in microglia--
100 implications for homeostasis, CNS autoimmunity and interferonopathies', *Curr Opin Neurobiol*,
101 36: 38-42.
102 González-Scarano, Francisco, and Julio Martín-García. 2005. 'The neuropathogenesis of AIDS', *Nature*
103 *Reviews Immunology*, 5: 69-81.
104 Gosselin, David, Dylan Skola, Nicole G. Coufal, Inge R. Holtman, Johannes C. M. Schlachetzki, Eniko
105 Sajti, Baptiste N. Jaeger, Carolyn O'Connor, Conor Fitzpatrick, Martina P. Pasillas, Monique
106 Pena, Amy Adair, David D. Gonda, Michael L. Levy, Richard M. Ransohoff, Fred H. Gage, and
107 Christopher K. Glass. 2017. 'An environment-dependent transcriptional network specifies
108 human microglia identity', *Science*, 356: eaal3222.
109 Gumbs, Stephanie B. H., Amber Berdenis van Berlekom, Raphael Kübler, Pauline J. Schipper, Lavina
110 Gharu, Marco P. Boks, Paul R. Ormel, Annemarie M. J. Wensing, Lot D. de Witte, and Monique
111 Nijhuis. 2022. "Characterization of HIV-1 Infection in Microglia-Containing Human Cerebral
112 Organoids." In *Viruses*.
113 Haenseler, W., S. N. Sansom, J. Buchrieser, S. E. Newey, C. S. Moore, F. J. Nicholls, S. Chintawar, C.
114 Schnell, J. P. Antel, N. D. Allen, M. Z. Cader, R. Wade-Martins, W. S. James, and S. A. Cowley.
115 2017. 'A Highly Efficient Human Pluripotent Stem Cell Microglia Model Displays a Neuronal-Co-
116 culture-Specific Expression Profile and Inflammatory Response', *Stem Cell Reports*, 8: 1727-42.
117 Hammond, Timothy R., Connor Dufort, Lasse Dissing-Olesen, Stefanie Giera, Adam Young, Alec
118 Wysoker, Alec J. Walker, Frederick Gergits, Michael Segel, James Nemesh, Samuel E. Marsh,
119 Arpiar Saunders, Evan Macosko, Florent Ginhoux, Jinmiao Chen, Robin J. M. Franklin, Xianhua
120 Piao, Steven A. McCarroll, and Beth Stevens. 2019. 'Single-Cell RNA Sequencing of Microglia
121 throughout the Mouse Lifespan and in the Injured Brain Reveals Complex Cell-State Changes',
122 *Immunity*, 50: 253-71.e6.
123 Hanisch, U. K. 2002. 'Microglia as a source and target of cytokines', *Glia*, 40: 140-55.
124 Hofer, Markus J., and Iain L. Campbell. 2013. 'Type I interferon in neurological disease—The devil from
125 within', *Cytokine & Growth Factor Reviews*, 24: 257-67.
126 Hur, J. Y., G. R. Frost, X. Wu, C. Crump, S. J. Pan, E. Wong, M. Barros, T. Li, P. Nie, Y. Zhai, J. C. Wang, J.
127 Tcw, L. Guo, A. McKenzie, C. Ming, X. Zhou, M. Wang, Y. Sagi, A. E. Renton, B. T. Esposito, Y.
128 Kim, K. R. Sadleir, I. Trinh, R. A. Rissman, R. Vassar, B. Zhang, D. S. Johnson, E. Masliah, P.
129 Greengard, A. Goate, and Y. M. Li. 2020. 'The innate immunity protein IFITM3 modulates γ-
130 secretase in Alzheimer's disease', *Nature*, 586: 735-40.

131 Israel, Sarah M., Shiva Hassanzadeh-Behbahani, Peter E. Turkeltaub, David J. Moore, Ronald J. Ellis, and
132 Xiong Jiang. 2019. 'Different roles of frontal versus striatal atrophy in HIV-associated
133 neurocognitive disorders', *Human Brain Mapping*, 40: 3010-26.
134 Izquierdo-Useros, Nuria, Maier Lorizate, Maria C. Puertas, Maria T. Rodriguez-Plata, Nadine Zangger,
135 Elina Erikson, Maria Pino, Itziar Erkizia, Bärbel Glass, Bonaventura Clotet, Oliver T. Keppler,
136 Amalio Telenti, Hans-Georg Kräusslich, and Javier Martinez-Picado. 2012. 'Siglec-1 Is a Novel
137 Dendritic Cell Receptor That Mediates HIV-1 Trans-Infection Through Recognition of Viral
138 Membrane Gangliosides', *PLOS Biology*, 10: e1001448.
139 Jeremiah, N., H. Ferran, K. Antoniadou, K. De Azevedo, J. Nikolic, M. Maurin, P. Benaroch, and N.
140 Manel. 2023. 'RELA tunes innate-like interferon I/III responses in human T cells', *J Exp Med*, 220.
141 Jiao, Yanmei, Tong Zhang, Rui Wang, Hongwei Zhang, Xiaojie Huang, Jiming Yin, Liguo Zhang, Xiaoning
142 Xu, and Hao Wu. 2012. 'Plasma IP-10 Is Associated with Rapid Disease Progression in Early HIV-
143 1 Infection', *Viral Immunology*, 25: 333-37.
144 Jin, M., R. Xu, L. Wang, M. M. Alam, Z. Ma, S. Zhu, A. C. Martini, A. Jadali, M. Bernabucci, P. Xie, K. Y.
145 Kwan, Z. P. Pang, E. Head, Y. Liu, R. P. Hart, and P. Jiang. 2022. 'Type-I-interferon signaling drives
146 microglial dysfunction and senescence in human iPSC models of Down syndrome and
147 Alzheimer's disease', *Cell Stem Cell*, 29: 1135-53.e8.
148 Kalter, D. C., M. Nakamura, J. A. Turpin, L. M. Baca, D. L. Hoover, C. Dieffenbach, P. Ralph, H. E.
149 Gendelman, and M. S. Meltzer. 1991. 'Enhanced HIV replication in macrophage colony-
150 stimulating factor-treated monocytes', *J Immunol*, 146: 298-306.
151 Kaul, M., J. Zheng, S. Okamoto, H. E. Gendelman, and S. A. Lipton. 2005. 'HIV-1 infection and AIDS:
152 consequences for the central nervous system', *Cell Death Differ*, 12 Suppl 1: 878-92.
153 Kaul, Marcus, Gwenn A. Garden, and Stuart A. Lipton. 2001. 'Pathways to neuronal injury and
154 apoptosis in HIV-associated dementia', *Nature*, 410: 988-94.
155 Koenig, S., H. E. Gendelman, J. M. Orenstein, M. C. Dal Canto, G. H. Pezeshkpour, M. Yungbluth, F.
156 Janotta, A. Aksamit, M. A. Martin, and A. S. Fauci. 1986. 'Detection of AIDS virus in
157 macrophages in brain tissue from AIDS patients with encephalopathy', *Science*, 233: 1089-93.
158 Kolb, Stefan A., Bernd Sporer, Fritz Lahrtz, Uwe Koedel, Hans-Walter Pfister, and Adriano Fontana.
159 1999. 'Identification of a T cell chemotactic factor in the cerebrospinal fluid of HIV-1-infected
160 individuals as interferon-γ inducible protein 10', *Journal of Neuroimmunology*, 93: 172-81.
161 Koyanagi, Y., S. Miles, R. T. Mitsuyasu, J. E. Merrill, H. V. Vinters, and I. S. Chen. 1987. 'Dual infection of
162 the central nervous system by AIDS viruses with distinct cellular tropisms', *Science*, 236: 819-22.
163 Kraft-Terry, Stephanie D., Shilpa J. Buch, Howard S. Fox, and Howard E. Gendelman. 2009. 'A Coat of
164 Many Colors: Neuroimmune Crosstalk in Human Immunodeficiency Virus Infection', *Neuron*, 64:
165 133-45.
166 Krivine, A., G. Force, J. Servan, A. Cabée, F. Rozenberg, L. Dighiero, F. Marguet, and P. Lebon. 1999.
167 'Measuring HIV-1 RNA and interferon-alpha in the cerebrospinal fluid of AIDS patients: insights
168 into the pathogenesis of AIDS Dementia Complex', *J Neurovirol*, 5: 500-6.
169 Kutsch, O., J. Oh, A. Nath, and E. N. Benveniste. 2000. 'Induction of the chemokines interleukin-8 and
170 IP-10 by human immunodeficiency virus type 1 tat in astrocytes', *J Virol*, 74: 9214-21.
171 Kutza, J., K. Fields, T. A. Grimm, and K. A. Clouse. 2002. 'Inhibition of HIV replication and macrophage
172 colony-stimulating factor production in human macrophages by antiretroviral agents', *AIDS Res*
173 *Hum Retroviruses*, 18: 619-25.

174 Kutza, Joseph, Lynne Crim, Steven Feldman, Mark P. Hayes, Marion Gruber, Judy Beeler, and Kathleen
175 A. Clouse. 2000. 'Macrophage Colony-Stimulating Factor Antagonists Inhibit Replication of HIV-
176 1 in Human Macrophages', *The Journal of Immunology*, 164: 4955.
177 Lancaster, Madeline A., and Juergen A. Knoblich. 2014. 'Generation of cerebral organoids from human
178 pluripotent stem cells', *Nature Protocols*, 9: 2329-40.
179 Lancaster, Madeline A., Magdalena Renner, Carol-Anne Martin, Daniel Wenzel, Louise S. Bicknell,
180 Matthew E. Hurles, Tessa Homfray, Josef M. Penninger, Andrew P. Jackson, and Juergen A.
181 Knoblich. 2013. 'Cerebral organoids model human brain development and microcephaly',
182 *Nature*, 501: 373-79.
183 Lee, Jeong Seok, and Eui-Cheol Shin. 2020. 'The type I interferon response in COVID-19: implications for
184 treatment', *Nature Reviews Immunology*, 20: 585-86.
185 Lei, Jie, Xiaowan Yin, Hong Shang, and Yongjun Jiang. 2019. 'IP-10 is highly involved in HIV infection',
186 *Cytokine*, 115: 97-103.
187 Letendre, S. L., E. R. Lanier, and J. A. McCutchan. 1999. 'Cerebrospinal fluid beta chemokine
188 concentrations in neurocognitively impaired individuals infected with human immunodeficiency
189 virus type 1', *J Infect Dis*, 180: 310-9.
190 Lew, Brandon J., Timothy J. McDermott, Alex I. Wiesman, Jennifer Neill, Mackenzie S. Mills, Kevin R.
191 Robertson, Howard S. Fox, Susan Swindells, and Tony W. Wilson. 2018. 'Neural dynamics of
192 selective attention deficits in HIV-associated neurocognitive disorder', *Neurology*, 91: e1860.
193 Li, Qingyun, and Ben A. Barres. 2018. 'Microglia and macrophages in brain homeostasis and disease',
194 *Nature Reviews Immunology*, 18: 225-42.
195 Li, Y., J. C. Kappes, J. A. Conway, R. W. Price, G. M. Shaw, and B. H. Hahn. 1991. 'Molecular
196 characterization of human immunodeficiency virus type 1 cloned directly from uncultured
197 human brain tissue: identification of replication-competent and -defective viral genomes',
198 *Journal of Virology*, 65: 3973-85.
199 Lindl, Kathryn A., David R. Marks, Dennis L. Kolson, and Kelly L. Jordan-Sciutto. 2010. 'HIV-Associated
200 Neurocognitive Disorder: Pathogenesis and Therapeutic Opportunities', *Journal of*
201 *Neuroimmune Pharmacology*, 5: 294-309.
202 Mackelprang, R. D., A. Filali-Mouhim, B. Richardson, F. Lefebvre, E. Katabira, A. Ronald, G. Gray, K. W.
203 Cohen, N. R. Klatt, T. Pecor, C. Celum, M. J. McElrath, S. M. Hughes, F. Hladik, M. J. Cameron,
204 and J. R. Lingappa. 2023. 'Upregulation of IFN-stimulated genes persists beyond the transitory
205 broad immunologic changes of acute HIV-1 infection', *iScience*, 26: 106454.
206 Maddison, D. C., and F. Giorgini. 2015. 'The kynurenine pathway and neurodegenerative disease',
207 *Semin Cell Dev Biol*, 40: 134-41.
208 Malpass, K. 2011. 'Neurodegenerative disease: the kynurenine pathway--promising new targets and
209 therapies for neurodegenerative disease', *Nat Rev Neurol*, 7: 417.
210 Marodon, Gilles, David Warren, Michael C. Filomio, and David N. Posnett. 1999. 'Productive infection of
211 double-negative T cells with HIV in vivo', *Proceedings of the National*
212 *Academy of Sciences*, 96: 11958.
213 McGlasson, Sarah, Alexa Jury, Andrew Jackson, and David Hunt. 2015. 'Type I interferon dysregulation
214 and neurological disease', *Nature Reviews Neurology*, 11: 515-23.
215 Merimsky, Ofer, Irith Reider-Groswasser, Moshe Inbar, and Samario Chaitchik. 1990. 'Interferon-
216 related mental deterioration and behavioral changes in patients with renal cell carcinoma',
217 *European Journal of Cancer and Clinical Oncology*, 26: 596-600.

218 Merrill, J. E., Y. Koyanagi, J. Zack, L. Thomas, F. Martin, and I. S. Chen. 1992. 'Induction of interleukin-1
219 and tumor necrosis factor alpha in brain cultures by human immunodeficiency virus type 1',
220 *Journal of Virology*, 66: 2217.
221 Min, A. K., B. Javidfar, R. Missall, D. Doanman, M. Durens, S. S. Vil, Z. Masih, M. Graziani, A. Mordelt, S.
222 Marro, L. de Witte, B. K. Chen, T. H. Swartz, and S. Akbarian. 2023. 'HIV-1 infection of
223 genetically engineered iPSC-derived central nervous system-engrafted microglia in a humanized
224 mouse model', *bioRxiv*.
225 Mitrasinovic, Olivera M., Grace V. Perez, FeiFei Zhao, Yuen Ling Lee, Clara Poon, and Greer M. Murphy.
226 2001. 'Overexpression of Macrophage Colony-stimulating Factor Receptor on Microglial Cells
227 Induces an Inflammatory Response*', *Journal of Biological Chemistry*, 276: 30142-49.
228 Moretti, S., S. Virtuoso, L. Sernicola, S. Farcomeni, M. T. Maggiorella, and A. Borsetti. 2021. 'Advances
229 in SIV/SHIV Non-Human Primate Models of NeuroAIDS', *Pathogens*, 10.
230 Nasr, N., A. A. Alshehri, T. K. Wright, M. Shahid, B. M. Heiner, A. N. Harman, R. A. Botting, K. J. Helbig,
231 M. R. Beard, K. Suzuki, A. D. Kelleher, P. Hertzog, and A. L. Cunningham. 2017. 'Mechanism of
232 Interferon-Stimulated Gene Induction in HIV-1-Infected Macrophages', *J Virol*, 91.
233 Ormel, Paul R., Renata Vieira de Sá, Emma J. van Bodegraven, Henk Karst, Oliver Harschnitz, Marjolein
234 A. M. Sneeboer, Lill Eva Johansen, Roland E. van Dijk, Nicky Scheefhals, Amber Berdenis van
235 Berlekom, Eduardo Ribes Martínez, Sandra Kling, Harold D. MacGillavry, Leonard H. van den
236 Berg, René S. Kahn, Elly M. Hol, Lot D. de Witte, and R. Jeroen Pasterkamp. 2018. 'Microglia
237 innately develop within cerebral organoids', *Nature Communications*, 9: 4167.
238 Paolicelli, Rosa C., Giulia Bolasco, Francesca Pagani, Laura Maggi, Maria Scianni, Patrizia Panzanelli,
239 Maurizio Giustetto, Tiago Alves Ferreira, Eva Guiducci, Laura Dumas, Davide Ragozzino, and
240 Cornelius T. Gross. 2011. 'Synaptic Pruning by Microglia Is Necessary for Normal Brain
241 Development', *Science*, 333: 1456.
242 Paşca, Anca M., Steven A. Sloan, Laura E. Clarke, Yuan Tian, Christopher D. Makinson, Nina Huber, Chul
243 Hoon Kim, Jin-Young Park, Nancy A. O'Rourke, Khoa D. Nguyen, Stephen J. Smith, John R.
244 Huguenard, Daniel H. Geschwind, Ben A. Barres, and Sergiu P. Paşca. 2015. 'Functional cortical
245 neurons and astrocytes from human pluripotent stem cells in 3D culture', *Nature Methods*, 12:
246 671-78.
247 Pavol, M. A., C. A. Meyers, J. L. Rexer, A. D. Valentine, P. J. Mattis, and M. Talpaz. 1995. 'Pattern of
248 neurobehavioral deficits associated with interferon alfa therapy for leukemia', *Neurology*, 45:
249 947-50.
250 Peluso, Michael J., Victor Valcour, Nittaya Phanuphak, Jintanat Ananworanich, James L. K. Fletcher,
251 Thep Chalermchai, Shelly J. Krebs, Merlin L. Robb, Joanna Hellmuth, Magnus Gisslén, Henrik
252 Zetterberg, Serena Spudich, Rv Search Rv254Search, and Search Study Teams. 2017. 'Immediate
253 initiation of cART is associated with lower levels of cerebrospinal fluid YKL-40, a marker of
254 microglial activation, in HIV-1 infection', *AIDS (London, England)*, 31: 247-52.
255 Perrella, O., P. B. Carreiri, A. Perrella, C. Sbreglia, F. Gorga, D. Guarnaccia, and G. Tarantino. 2001.
256 'Transforming growth factor beta-1 and interferon-alpha in the AIDS dementia complex (ADC):
257 possible relationship with cerebral viral load?', *Eur Cytokine Netw*, 12: 51-5.
258 Phetsouphanh, Chansavath, David R. Darley, Daniel B. Wilson, Annett Howe, C. Mee Ling Munier,
259 Sheila K. Patel, Jennifer A. Juno, Louise M. Burrell, Stephen J. Kent, Gregory J. Dore, Anthony D.
260 Kelleher, and Gail V. Matthews. 2022. 'Immunological dysfunction persists for 8 months
261 following initial mild-to-moderate SARS-CoV-2 infection', *Nature Immunology*, 23: 210-16.

262 Platanias, Leonidas C. 2005. 'Mechanisms of type-I- and type-II-interferon-mediated signalling', *Nature*
263 *Reviews Immunology*, 5: 375-86.
264 Qian, Xuyu, Yijing Su, Christopher D. Adam, Andre U. Deutschmann, Sarshan R. Pather, Ethan M.
265 Goldberg, Kenong Su, Shiying Li, Lu Lu, Fadi Jacob, Phuong T. T. Nguyen, Sooyoung Huh, Ahmet
266 Hoke, Sarah E. Swinford-Jackson, Zhexing Wen, Xiaosong Gu, R. Christopher Pierce, Hao Wu,
267 Lisa A. Briand, H. Isaac Chen, John A. Wolf, Hongjun Song, and Guo-li Ming. 2020. 'Sliced Human
268 Cortical Organoids for Modeling Distinct Cortical Layer Formation', *Cell Stem Cell*, 26: 766-81.e9.
269 Quadrato, Giorgia, Tuan Nguyen, Evan Z. Macosko, John L. Sherwood, Sung Min Yang, Daniel R. Berger,
270 Natalie Maria, Jorg Scholvin, Melissa Goldman, Justin P. Kinney, Edward S. Boyden, Jeff W.
271 Lichtman, Ziv M. Williams, Steven A. McCarroll, and Paola Arlotta. 2017. 'Cell diversity and
272 network dynamics in photosensitive human brain organoids', *Nature*, 545: 48-53.
273 Rai, Mohammad A., Jason Hammonds, Mario Pujato, Christopher Mayhew, Krishna Roskin, and Paul
274 Spearman. 2020. 'Comparative analysis of human microglial models for studies of HIV
275 replication and pathogenesis', *Retrovirology*, 17: 35.
276 Raison, Charles L., Marina Demetrashvili, Lucile Capuron, and Andrew H. Miller. 2005.
277 'Neuropsychiatric Adverse Effects of Interferon-α', *CNS Drugs*, 19: 105-23.
278 Ramesh, Geeta, Andrew G. MacLean, and Mario T. Philipp. 2013. 'Cytokines and Chemokines at the
279 Crossroads of Neuroinflammation, Neurodegeneration, and Neuropathic Pain', *Mediators of*
280 *Inflammation*, 2013: 480739.
281 Rappaport, Jay, Jeymohan Joseph, Sidney Croul, Guillermo Alexander, Luis Del Valle, Shohreh Amini,
282 and Kamel Khalili. 1999. 'Molecular pathway involved in HIV-1-induced CNS pathology: role of
283 viral regulatory protein, Tat', *Journal of Leukocyte Biology*, 65: 458-65.
284 Rho, M. B., S. Wesselingh, J. D. Glass, J. C. McArthur, S. Choi, J. Griffin, and W. R. Tyor. 1995. 'A
285 Potential Role for Interferon-α in the Pathogenesis of HIV-Associated Dementia', *Brain,*
286 *Behavior, and Immunity*, 9: 366-77.
287 Roy, Ethan R., Gabriel Chiu, Sanming Li, Nicholas E. Propson, Rupa Kanchi, Baiping Wang, Cristian
288 Coarfa, Hui Zheng, and Wei Cao. 2022. 'Concerted type I interferon signaling in microglia and
289 neural cells promotes memory impairment associated with amyloid β plaques', *Immunity*, 55:
290 879-94.e6.
291 Roy, Ethan R., Baiping Wang, Ying-wooi Wan, Gabriel Chiu, Allysa Cole, Zhuoran Yin, Nicholas E.
292 Propson, Yin Xu, Joanna L. Jankowsky, Zhandong Liu, Virginia M. Y. Lee, John Q. Trojanowski,
293 Stephen D. Ginsberg, Oleg Butovsky, Hui Zheng, and Wei Cao. 2020. 'Type I interferon response
294 drives neuroinflammation and synapse loss in Alzheimer disease', *The Journal of Clinical*
295 *Investigation*, 130: 1912-30.
296 Ruhanya, Vurayai, Graeme B. Jacobs, Shalena Naidoo, Robert H. Paul, John A. Joska, Soraya Seedat,
297 George Nyandoro, Susan Engelbrecht, and Richard H. Glashoff. 2021. 'Impact of Plasma IP-
298 10/CXCL10 and RANTES/CCL5 Levels on Neurocognitive Function in HIV Treatment-Naive
299 Patients', *AIDS Research and Human Retroviruses*.
300 Ryan, Sean K., Michael V. Gonzalez, James P. Garifallou, Frederick C. Bennett, Kimberly S. Williams,
301 Nathaniel P. Sotuyo, Eugene Mironets, Kieona Cook, Hakon Hakonarson, Stewart A. Anderson,
302 and Kelly L. Jordan-Sciutto. 2020. 'Neuroinflammation and EIF2 Signaling Persist despite
303 Antiretroviral Treatment in an hiPSC Tri-culture Model of HIV Infection', *Stem Cell Reports*, 14:
304 703-16.

305 Sacktor, N., R. L. Skolasky, E. Seaberg, C. Munro, J. T. Becker, E. Martin, A. Ragin, A. Levine, and E.
306 Miller. 2016. 'Prevalence of HIV-associated neurocognitive disorders in the Multicenter AIDS
307 Cohort Study', *Neurology*, 86: 334-40.
308 Sacktor, Ned. 2018. 'Changing clinical phenotypes of HIV-associated neurocognitive disorders', *Journal*
309 *of NeuroVirology*, 24: 141-45.
310 Sanna, Pietro Paolo, Yu Fu, Eliezer Masliah, Celine Lefebvre, and Vez Repunte-Canonigo. 2021. 'Central
311 nervous system (CNS) transcriptomic correlates of human immunodeficiency virus (HIV) brain
312 RNA load in HIV-infected individuals', *Scientific Reports*, 11: 12176.
313 Schwarcz, R., and T. W. Stone. 2017. 'The kynurenine pathway and the brain: Challenges, controversies
314 and promises', *Neuropharmacology*, 112: 237-47.
315 Simioni, S., M. Cavassini, J. M. Annoni, A. Rimbault Abraham, I. Bourquin, V. Schiffer, A. Calmy, J. P.
316 Chave, E. Giacobini, B. Hirschel, and R. A. Du Pasquier. 2010. 'Cognitive dysfunction in HIV
317 patients despite long-standing suppression of viremia', *Aids*, 24: 1243-50.
318 Sloan, Steven A., Jimena Andersen, Anca M. Paşca, Fikri Birey, and Sergiu P. Paşca. 2018. 'Generation
319 and assembly of human brain region–specific three-dimensional cultures', *Nature Protocols*, 13:
320 2062-85.
321 Smith, Amy M., Hannah M. Gibbons, Robyn L. Oldfield, Peter M. Bergin, Edward W. Mee, Maurice A.
322 Curtis, Richard L. M. Faull, and Mike Dragunow. 2013. 'M-CSF increases proliferation and
323 phagocytosis while modulating receptor and transcription factor expression in adult human
324 microglia', *Journal of Neuroinflammation*, 10: 859.
325 Solomon, Isaac H., Sukrutha Chettimada, Vikas Misra, David R. Lorenz, Robert J. Gorelick, Benjamin B.
326 Gelman, Susan Morgello, and Dana Gabuzda. 2020. 'White Matter Abnormalities Linked to
327 Interferon, Stress Response, and Energy Metabolism Gene Expression Changes in Older HIV-
328 Positive Patients on Antiretroviral Therapy', *Molecular Neurobiology*, 57: 1115-30.
329 Song, Wilbur M., and Marco Colonna. 2018. 'The identity and function of microglia in
330 neurodegeneration', *Nature Immunology*, 19: 1048-58.
331 Sreeram, S., F. Ye, Y. Garcia-Mesa, K. Nguyen, A. El Sayed, K. Leskov, and J. Karn. 2022. 'The potential
332 role of HIV-1 latency in promoting neuroinflammation and HIV-1-associated neurocognitive
333 disorder', *Trends Immunol*, 43: 630-39.
334 Valverde-Villegas, J. M., R. M. de Medeiros, J. H. Ellwanger, B. R. Santos, M. G. Melo, S. E. M. Almeida,
335 and J. A. B. Chies. 2018. 'High CXCL10/IP-10 levels are a hallmark in the clinical evolution of the
336 HIV infection', *Infect Genet Evol*, 57: 51-58.
337 van Marle, G., S. Henry, T. Todoruk, A. Sullivan, C. Silva, S. B. Rourke, J. Holden, J. C. McArthur, M. J.
338 Gill, and C. Power. 2004. 'Human immunodeficiency virus type 1 Nef protein mediates neural
339 cell death: a neurotoxic role for IP-10', *Virology*, 329: 302-18.
340 Vaughan-Jackson, Alun, Szymon Stodolak, Kourosh H. Ebrahimi, Cathy Browne, Paul K. Reardon,
341 Elisabete Pires, Javier Gilbert-Jaramillo, Sally A. Cowley, and William S. James. 2021.
342 'Differentiation of human induced pluripotent stem cells to authentic macrophages using a
343 defined, serum-free, open-source medium', *Stem Cell Reports*, 16: 1735-48.
344 Velasco, Silvia, Amanda J. Kedaigle, Sean K. Simmons, Allison Nash, Marina Rocha, Giorgia Quadrato,
345 Bruna Paulsen, Lan Nguyen, Xian Adiconis, Aviv Regev, Joshua Z. Levin, and Paola Arlotta. 2019.
346 'Individual brain organoids reproducibly form cell diversity of the human cerebral cortex',
347 *Nature*, 570: 523-27.

348 Vodyanik, Maxim A., James A. Thomson, and Igor I. Slukvin. 2006. 'Leukosialin (CD43) defines
349 hematopoietic progenitors in human embryonic stem cell differentiation cultures', *Blood*, 108:
350 2095-105.
351 Wichers, M. C., G. H. Koek, G. Robaeys, A. J. Praamstra, and M. Maes. 2005. 'Early increase in
352 vegetative symptoms predicts IFN-α-induced cognitive-depressive changes', *Psychological*
353 *Medicine*, 35: 433-41.
354 Wiley, C. A., R. A. Steinman, and Q. Wang. 2023. 'Innate immune activation without immune cell
355 infiltration in brains of murine models of Aicardi-Goutières Syndrome', *Brain Pathol*, 33:
356 e13118.
357 Woodburn, B. M., K. Kanchi, S. Zhou, N. Colaianni, S. B. Joseph, and R. Swanstrom. 2022.
358 'Characterization of Macrophage-Tropic HIV-1 Infection of Central Nervous System Cells and the
359 Influence of Inflammation', *J Virol*, 96: e0095722.
360 Xu, R., A. J. Boreland, X. Li, C. Erickson, M. Jin, C. Atkins, Z. P. Pang, B. P. Daniels, and P. Jiang. 2021.
361 'Developing human pluripotent stem cell-based cerebral organoids with a controllable microglia
362 ratio for modeling brain development and pathology', *Stem Cell Reports*, 16: 1923-37.
363 Yoon, Se-Jin, Lubayna S. Elahi, Anca M. Pașca, Rebecca M. Marton, Aaron Gordon, Omer Revah, Yuki
364 Miura, Elisabeth M. Walczak, Gwendolyn M. Holdgate, H. Christina Fan, John R. Huguenard,
365 Daniel H. Geschwind, and Sergiu P. Pașca. 2019. 'Reliability of human cortical organoid
366 generation', *Nature Methods*, 16: 75-78.
367 Yu, H., A. B. Rabson, M. Kaul, Y. Ron, and J. P. Dougherty. 1996. 'Inducible human immunodeficiency
368 virus type 1 packaging cell lines', *Journal of Virology*, 70: 4530-37.
369 Zou, Zhongcheng, Ashley Chastain, Susan Moir, Jennifer Ford, Kathryn Trandem, Elena Martinelli,
370 Claudia Cicala, Paul Crocker, James Arthos, and Peter D. Sun. 2011. 'Siglecs Facilitate HIV-1
371 Infection of Macrophages through Adhesion with Viral Sialic Acids', *PLoS One*, 6: e24559.
372

373

374 **FIGURE LEGENDS**

375

376 **Figure 1: Human microglia are efficiently generated from induced pluripotent stem cells**

377 (A) Representative brightfield images showing the induction of iPSCs to mesodermal yolk sac embryoid
378 bodies (EB) and then to primitive microglia progenitor cells (PMPs) and microglia.

379 (B) Representative confocal images of PMPs expressing the yolk sac marker CD235 and the
380 hematopoietic progenitor cell marker CD43 in the 03SF cell line.

381 (C) RT–qPCR analysis of *IBA1* and *P2RY12* mRNA expression in iPSCs and iPSC-derived microglia;
382 n=3 cell lines (03SF, CD06, CD52); t test; data are presented as the mean ± SEM.

383 (D) Representative confocal images of microglia stained for the microglial markers IBA1, P2Y12,
384 CX3CR1, TMEM119, and PU1 and costained with DAPI; n = 3 cell lines (03SF, CD06, CD52).

385 (E) Representative confocal image of a microglial cell displaying ramified morphology after 4 weeks of
386 coculture with neurons.

387 (F) Representative confocal images of a 03SF cell line iPSC-derived microglial neuronal coculture
388 stained for neurons (MAP2), synapses (SYN1), and microglia (IBA1). (F1 and F2) Orthogonal view of
389 microglial (IBA1+) processes colocalized with neuronal dendrites (MAP2) and synapses (SYN1).

390 (G) RT–qPCR analysis of *CD4* and *CCR5* mRNA from iPSCs and microglia; n=3 cell lines (03SF,
391 CD06, CD52); t test; data are presented as the mean ± SEM.

392

393

394 **Figure 2: HIV-1-infected microglia exhibit productive infection, activation, and dysregulated**
395 **cytokine/chemokine production**

396 (A) RT–qPCR analysis of viral *gag/pol* mRNA after infection with HIV-1 JRFL in microglia monocultures;
397 n=3 independent infections of 03SF line iPSC-derived microglia.

398 (B) ELISA analysis of secreted p24 in the culture supernatant of microglia infected with HIV-1 JR-FL
399 reveals productive infection; n=3 independent infections of 03SF iPSC-derived microglia.

400 (C) RT–qPCR analysis of *IL1β, TNFα*, and *IL-6* mRNA at days 16 and 23 post infection with HIV-1
401 JRFL; n=3 independent infections of 03SF iPSC-derived microglia, t test; data are presented as the
402 mean ± SEM.
403 (D) RT–qPCR analysis of *CCL2, CCL3*, and *CCL5* mRNA at days 16 and 23 post infection with HIV-1
404 JRFL; n=3 independent infections of 03SF iPSC-derived microglia.
405 (E) RT–qPCR analysis of *IBA1* and *P2RY12* mRNA at days 16 and 23 post infection with HIV-1 JRFL;
406 n=3 independent infections of 03SF iPSC-derived microglia.
407 (F) Luminex cytokine/chemokine analysis of secreted M-CSF and IP-10/CXCL10 culture supernatant
408 from HIV-1 JRFL-infected microglia; n=3 independent infections of 03SF microglia, two-way ANOVA;
409 data are presented as the mean ± SEM.
410 (G) Representative confocal images of nucleocapsid protein p24 staining in HIV-1 JRFL-infected 03SF-
411 derived microglia ($IBA1^+$).
412
413 **Figure 3: HIV-1-infected microglia exhibit productive infection, activation, and dysregulated**
414 **cytokine/chemokine production**
415 (A) RT–qPCR analysis of viral *gag/pol* mRNA at days 9, 16, 23, and 30 post infection with HIV-1 JRFL
416 and HIV-1 YU2; n=3 independent infections of CD06 iPSC-derived microglia. t test
417 (B) ELISA analysis of secreted p24 in the culture supernatant of microglia infected with HIV-1 JRFL and
418 HIV-1 YU2 at days 9, 15, 21, and 27 reveals productive infection; n=3 independent infections of CD06
419 iPSC-derived microglia.
420 (C) RT–qPCR analysis of *IL1β* and *TNFα* mRNA at days 9, 16, 23, and 30 post infection with HIV-1
421 JRFL and HIV-1 YU2; n=3 independent infections of CD06 iPSC-derived microglia.
422 (D) RT–qPCR analysis of *CCL2* and *CCL3* mRNA at days 9, 16, 23, and 30 post infection with HIV-1
423 JRFL and HIV-1 YU2; n=3 independent infections of CD06 iPSC-derived microglia.
424 (E) RT–qPCR analysis of *IBA1* and *P2RY12* mRNA at days 9, 16, 23, and 30 post infection with HIV-1
425 JRFL and HIV-1 YU2; n=3 independent infections of CD06 iPSC-derived microglia.

426 **Figure 4: HIV-1 causes enrichment of type I interferon signaling pathways and sustained**
427 **interferon activation**
428 (A) A volcano plot illustrating differentially expressed genes (DEGs) in HIV-1 JRFL-infected vs mock-
429 infected microglia on day 16 post infection; n=3 independent infections of 03SF line iPSC-derived
430 microglia.
431 (B) GSEA plot showing enrichment of IFNα-responsive genes in HIV-1 JRFL-infected vs mock-infected
432 microglia on day 16 post infection (NES, normalized enrichment score; FDR, false discovery rate).
433 (C) Gene Ontology (GO) analysis of upregulated DEGs in HIV-1 JRFL vs mock-infected microglia on
434 day 16 post infection; n=3 independent infections of 03SF microglia.
435 (D) Gene Ontology (GO) analysis of downregulated DEGs in HIV-1 JRFL vs mock-infected microglia on
436 day 16 post infection; n=3 independent infections of 03SF microglia.
437 (E) A heatmap illustrating significant upregulation of interferon-stimulated genes in HIV-1-infected vs
438 mock-infected microglia on day 16 post infection; n=3 independent infections of 03SF microglia.
439 (F) A heatmap illustrating SIGLEC gene expression in HIV-1-infected vs mock-infected microglia on day
440 16 post infection; n=3 independent infections of 03SF microglia.
441 (G) RT–qPCR analysis of *CXCL10*, *RSAD2*, *ISG15*, and *IDO1* mRNA from HIV-1 JRFL-infected vs
442 mock-infected microglia at days 16 and 23 post infection; n = 3 independent infections of 03SF iPSC-
443 derived microglia, t test; *$p < 0.05$, **$p < 0.01$, ***$p < 0.001$; data are presented as the mean ± SEM.
444 (H) RT–qPCR analysis of *CXCL10* and *RSAD2* mRNA from HIV-1 JRFL- and HIV-1 YU2-infected and
445 mock-infected microglia at days 16 and 23 post infection; n = 4 independent infections of CD06 iPSC-
446 derived microglia, t test; *$p < 0.05$, **$p < 0.01$, ***$p < 0.001$; data are presented as the mean ± SEM.
447
448 **Figure 5: HIV-1-infected microglia incorporate into sliced cerebral organoids**
449 (A) Representative confocal images of a day 144 organoid with neurons ($MAP2^+$), astrocytes ($GFAP^+$),
450 and microglia ($IBA1^+$).

451 (B) Representative confocal images of day 144 organoids 14 days after the addition of HIV-1 JRFL-
452 infected or mock-infected microglia; (B1) shows a high-magnification image of HIV-1-infected microglia
453 from (B).
454 (C) High-magnification image of a single HIV-1-infected microglial cell within a sliced organoid.
455 (D) RT–qPCR of *gag/pol* mRNA from HIV-1 JRFL-infected or mock-infected microglia organoids on day
456 14; n=3 independent infections of 03SF microglia; one-tailed t test; ****P<0.001; error bars represent
457 SEM.
458 (E) ELISA analysis of secreted p24 in culture supernatant from HIV-1 JRFL-infected or mock-infected
459 microglia organoid day 14; n=3 independent infections of 03SF microglia; one-tailed t test; **p<0.01;
460 data are presented as the mean ± SEM.
461 (F) RT–qPCR analysis of *ISG15*, *RSAD2*, *IFITM3*, *MX1*, *IFI44*, and *IFI27* mRNA from HIV-1 JRFL-
462 infected or mock-infected microglia organoids on day 14; n=3 independent infections of 03SF microglia;
463 one-tailed t test; *p < 0.05, **p < 0.01, ***p < 0.001; data are presented as the mean ± SEM.
464
465 **Figure S1: Microglial RT-qPCR analysis**
466 (A) RT–qPCR analysis of *IBA1* and *P2RY12* mRNA expression in iPSCs and iPSC-derived microglia;
467 n=3 cell lines (03SF, CD06, CD52) and 3 biological replicates/line; t test; data are presented as the
468 mean ± SEM.
469 (B) RT–qPCR analysis of *CD4* and *CCR5* mRNA expression in iPSCs and iPSC-derived microglia; n=3
470 cell lines (03SF, CD06, CD52) and 3 biological replicates/line; t test; data are presented as the mean ±
471 SEM.
472
473 **Figure S2: PCR analysis of 2-LTR circles**
474 (A) A schematic representation of HIV-1 structure.
475 (B) A schematic representation of an HIV-1 2-LTR circle.
476 (C) PCR analysis of 2-LTR circles on day 4 post HIV-1 JRFL infection and mock infection.

477

478 **Figure S3: RNA-seq analysis of HIV-1 JRFL- vs mock-infected 03SF microglia**

479 (A) A PCA plot of RNA-seq data collected from HIV-1 JRFL-infected microglia vs mock-infected

480 microglia on day 16; n=3 independent infections of 03SF microglia.

481 (B) A REVIGO treemap indicating major dysregulated pathways from gene ontology (GO) analysis of

482 HIV-1 JRFL-infected microglia vs mock-infected microglia on day 16; n=3 independent infections of

483 03SF microglia.

484

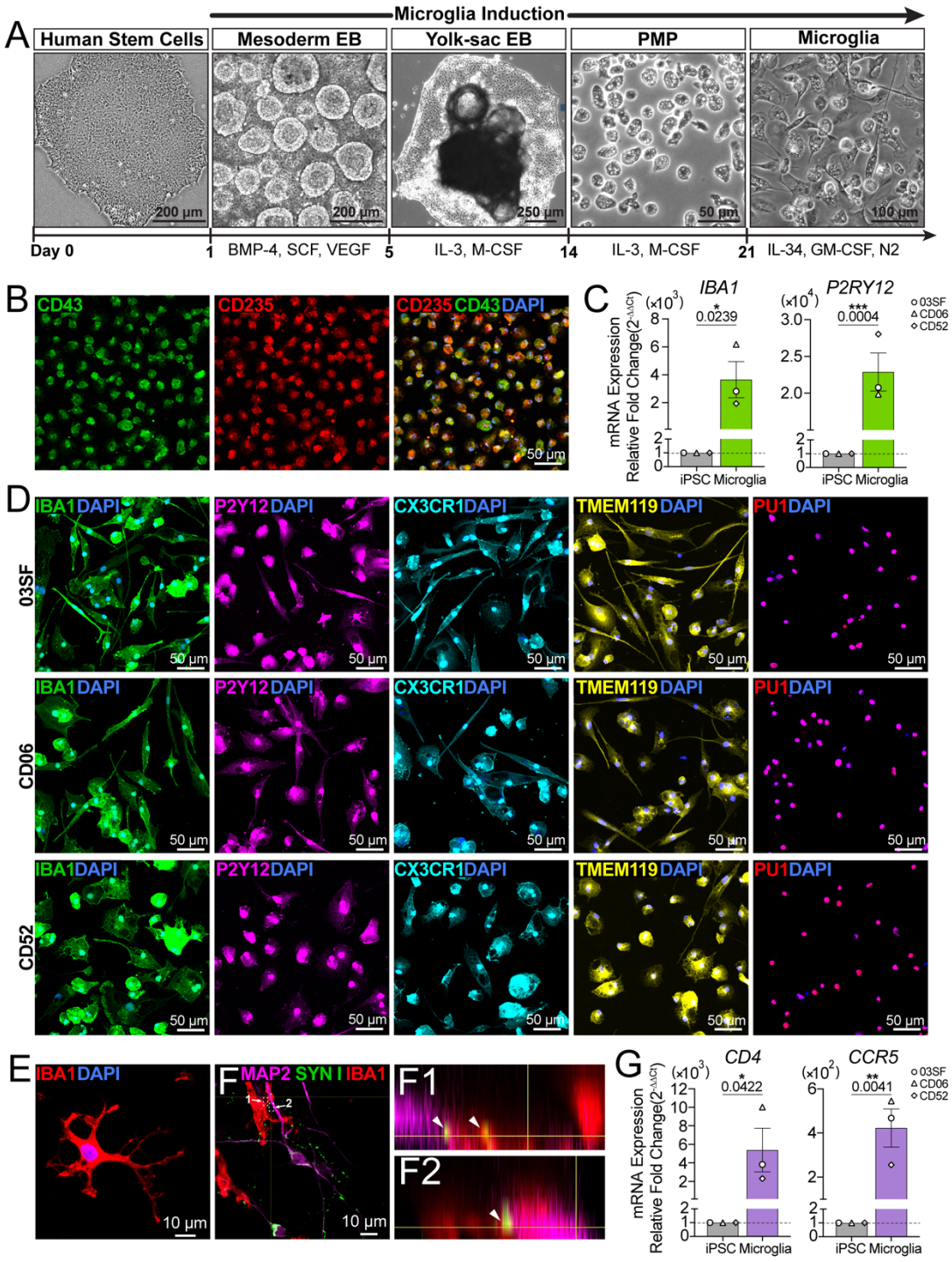
A
Microglia Induction
Human Stem Cells
Mesoderm EB
Yolk-sac EB
PMP
Microglia
200 µm
200 µm
250 µm
50 µm
100 µm
Day 0
1
BMP-4, SCF, VEGF
5
IL-3, M-CSF
14
IL-3, M-CSF
21
IL-34, GM-CSF, N2
B
CD43
CD235
CD235 CD43 DAPI
50 µm
C
IBA1
P2RY12
mRNA Expression Relative Fold Change(2^-ΔΔCt)
(×10^3)
(×10^4)
0.0239
0.0004
03SF
CD06
CD52
iPSC Microglia
iPSC Microglia
D
03SF
CD06
CD52
IBA1 DAPI
P2Y12 DAPI
CX3CR1 DAPI
TMEM119 DAPI
PU1 DAPI
50 µm
E
IBA1 DAPI
10 µm
F
MAP2 SYN I IBA1
10 µm
F1
F2
G
CD4
CCR5
mRNA Expression Relative Fold Change(2^-ΔΔCt)
(×10^3)
(×10^2)
0.0422
0.0041
03SF
CD06
CD52
iPSC Microglia
iPSC Microglia

Figure 1

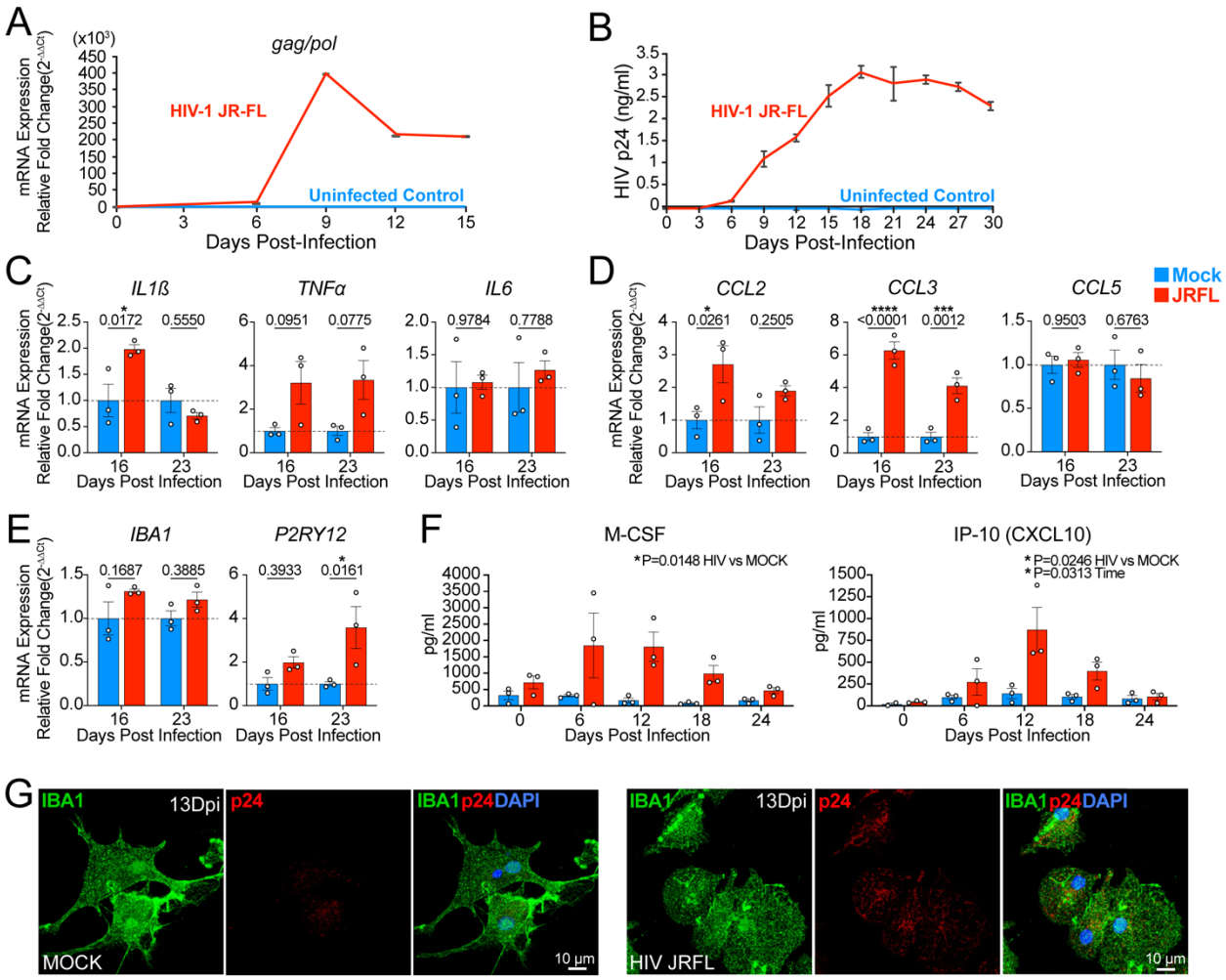
A
gag/pol
HIV-1 JR-FL
Uninfected Control
mRNA Expression Relative Fold Change(2-ΔΔCt)
Days Post-Infection
B
HIV-1 JR-FL
Uninfected Control
HIV p24 (ng/ml)
Days Post-Infection
C
IL1ß
TNFα
IL6
D
CCL2
CCL3
CCL5
Mock
JRFL
E
IBA1
P2RY12
F
M-CSF
*P=0.0148 HIV vs MOCK
IP-10 (CXCL10)
* P=0.0246 HIV vs MOCK
* P=0.0313 Time
pg/ml
Days Post Infection
G
IBA1
13Dpi
p24
IBA1p24DAPI
MOCK
HIV JRFL
10 µm

Figure 2

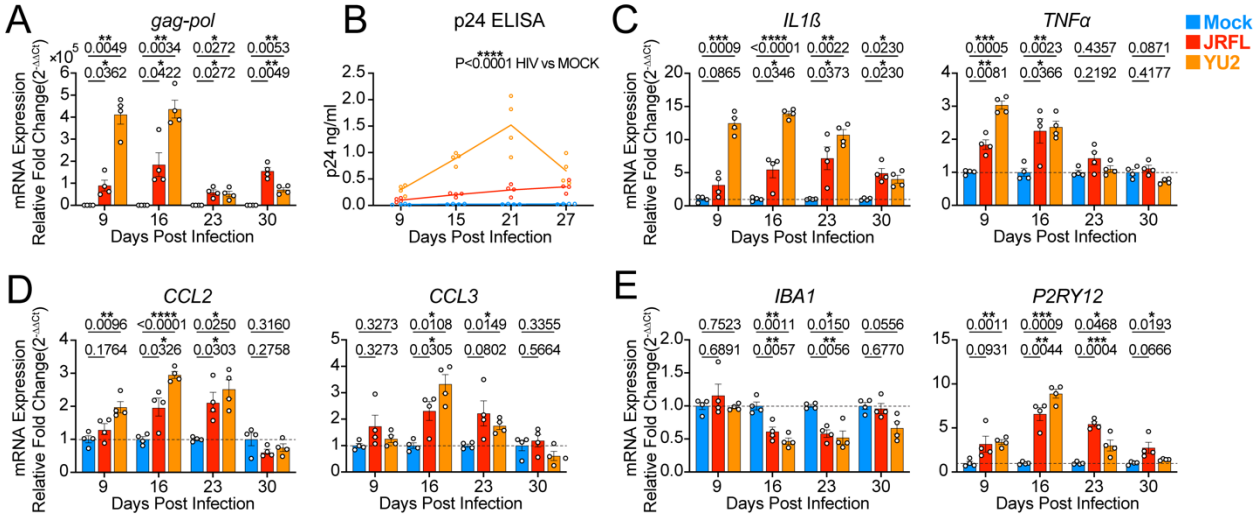
A
gag-pol
mRNA Expression
Relative Fold Change(2^-ΔΔCt)
Days Post Infection
B
p24 ELISA
P<0.0001 HIV vs MOCK
p24 ng/ml
Days Post Infection
C
IL1ß
TNFα
Mock
JRFL
YU2
D
CCL2
CCL3
E
IBA1
P2RY12

Figure 3

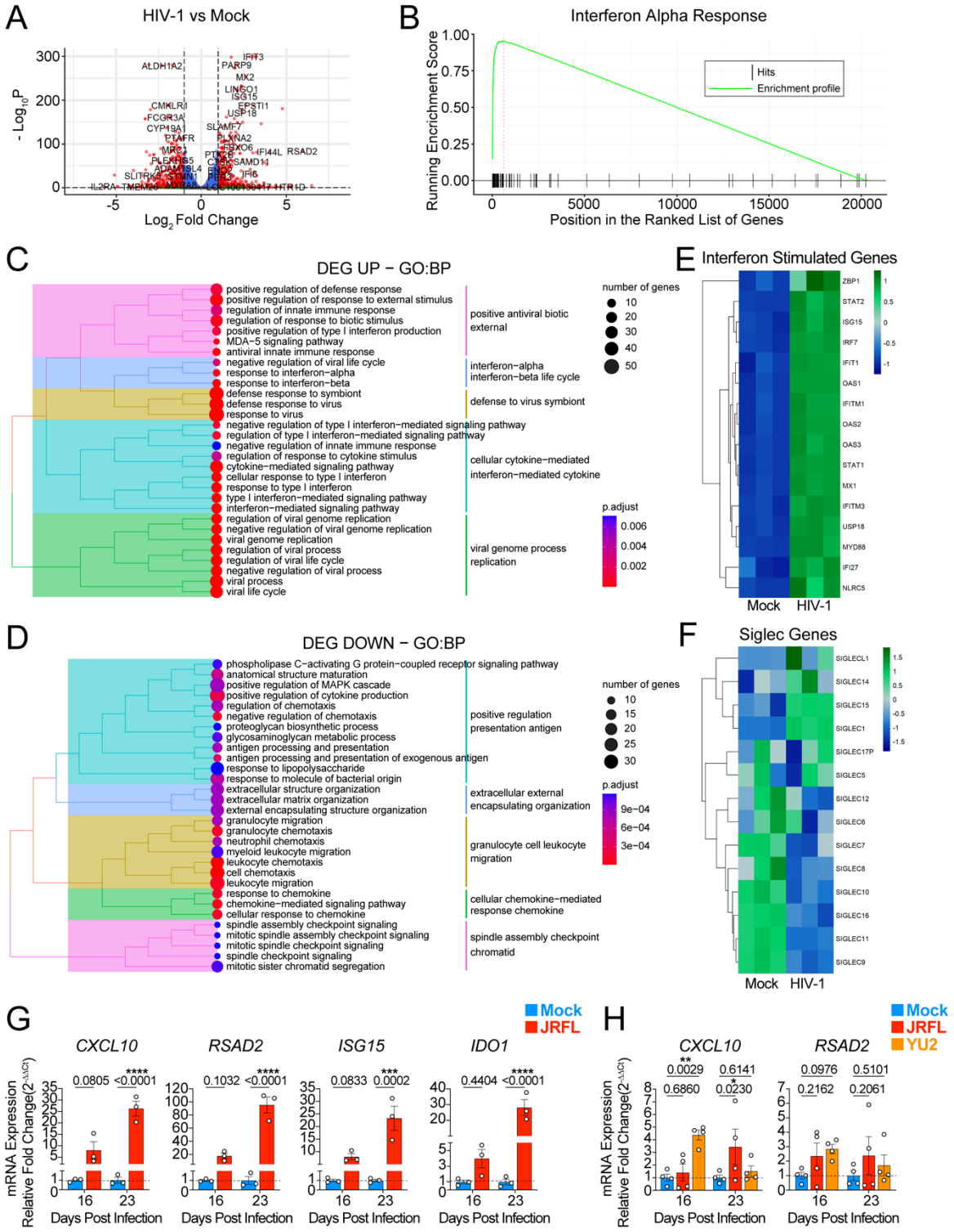
A
HIV-1 vs Mock
- Log10 P
Log2 Fold Change
B
Interferon Alpha Response
Running Enrichment Score
Hits
Enrichment profile
Position in the Ranked List of Genes
C
DEG UP − GO:BP
positive regulation of defense response
positive regulation of response to external stimulus
regulation of innate immune response
regulation of response to biotic stimulus
positive regulation of type I interferon production
MDA−5 signaling pathway
antiviral innate immune response
negative regulation of viral life cycle
response to interferon−alpha
response to interferon−beta
defense response to symbiont
defense response to virus
response to virus
negative regulation of type I interferon−mediated signaling pathway
regulation of type I interferon−mediated signaling pathway
negative regulation of innate immune response
regulation of response to cytokine stimulus
cytokine−mediated signaling pathway
cellular response to type I interferon
response to type I interferon
type I interferon−mediated signaling pathway
interferon−mediated signaling pathway
regulation of viral genome replication
negative regulation of viral genome replication
viral genome replication
regulation of viral process
regulation of viral life cycle
negative regulation of viral process
viral process
viral life cycle
positive antiviral biotic
external
interferon−alpha
interferon−beta life cycle
defense to virus symbiont
cellular cytokine−mediated
interferon−mediated cytokine
viral genome process
replication
number of genes
p.adjust
E
Interferon Stimulated Genes
ZBP1
STAT2
ISG15
IRF7
IFIT1
OAS1
IFITM1
OAS2
OAS3
STAT1
MX1
IFITM3
USP18
MYD88
IFI27
NLRC5
Mock
HIV-1
D
DEG DOWN − GO:BP
phospholipase C−activating G protein−coupled receptor signaling pathway
anatomical structure maturation
positive regulation of MAPK cascade
positive regulation of cytokine production
regulation of chemotaxis
negative regulation of chemotaxis
proteoglycan biosynthetic process
glycosaminoglycan metabolic process
antigen processing and presentation
antigen processing and presentation of exogenous antigen
response to lipopolysaccharide
response to molecule of bacterial origin
extracellular structure organization
extracellular matrix organization
external encapsulating structure organization
granulocyte migration
granulocyte chemotaxis
neutrophil chemotaxis
myeloid leukocyte migration
leukocyte chemotaxis
cell chemotaxis
leukocyte migration
response to chemokine
chemokine−mediated signaling pathway
cellular response to chemokine
spindle assembly checkpoint signaling
mitotic spindle assembly checkpoint signaling
mitotic spindle checkpoint signaling
spindle checkpoint signaling
mitotic sister chromatid segregation
positive regulation
presentation antigen
extracellular external
encapsulating organization
granulocyte cell leukocyte
migration
cellular chemokine−mediated
response chemokine
spindle assembly checkpoint
chromatid
number of genes
p.adjust
F
Siglec Genes
SIGLECL1
SIGLEC14
SIGLEC15
SIGLEC1
SIGLEC17P
SIGLEC5
SIGLEC12
SIGLEC6
SIGLEC7
SIGLEC8
SIGLEC10
SIGLEC16
SIGLEC11
SIGLEC9
Mock
HIV-1
G
Mock
JRFL
CXCL10
RSAD2
ISG15
IDO1
mRNA Expression
Relative Fold Change(2^-ΔΔCt)
Days Post Infection
H
Mock
JRFL
YU2
CXCL10
RSAD2
mRNA Expression
Relative Fold Change(2^-ΔΔCt)
Days Post Infection

Figure 4

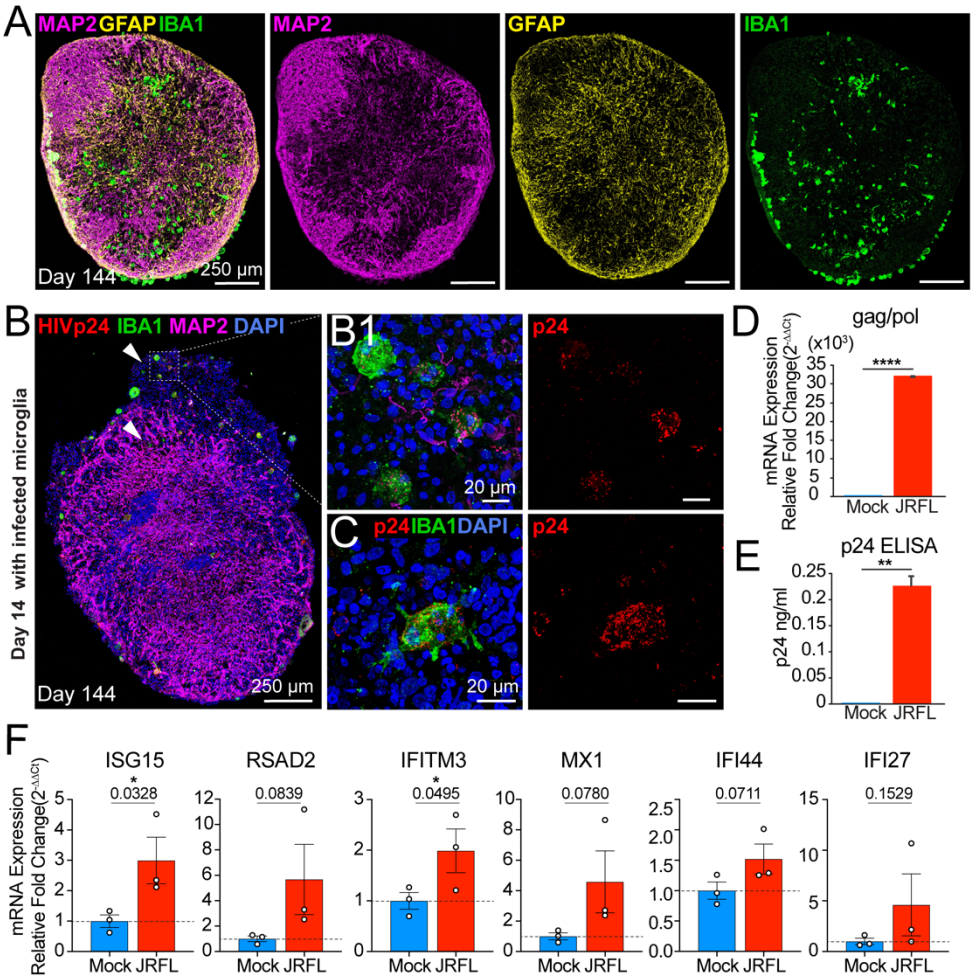
A
MAP2 GFAP IBA1
MAP2
GFAP
IBA1
Day 144
250 µm
B
HIV p24 IBA1 MAP2 DAPI
Day 14 with infected microglia
Day 144
250 µm
B1
p24
20 µm
C
p24 IBA1 DAPI
p24
20 µm
D
gag/pol
(x10³)
mRNA Expression Relative Fold Change(2^-ΔΔCt)
****
Mock JRFL
E
p24 ELISA
**
p24 ng/ml
Mock JRFL
F
ISG15
RSAD2
IFITM3
MX1
IFI44
IFI27
mRNA Expression Relative Fold Change(2^-ΔΔCt)
0.0328
0.0839
0.0495
0.0780
0.0711
0.1529
Mock JRFL

Figure 5

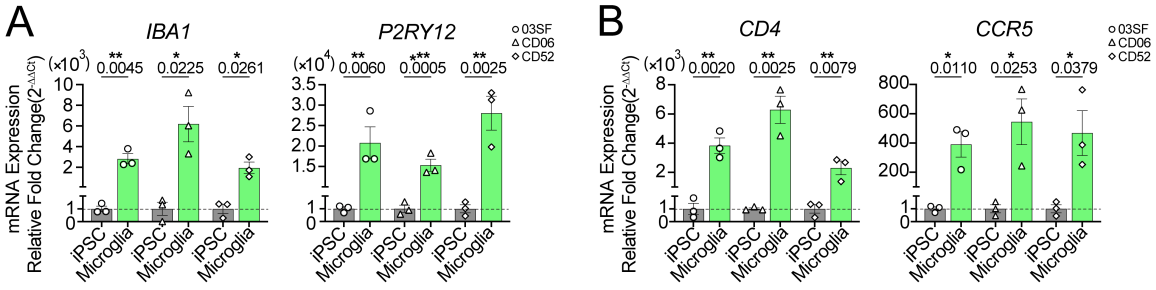

Supplemental Figure 1

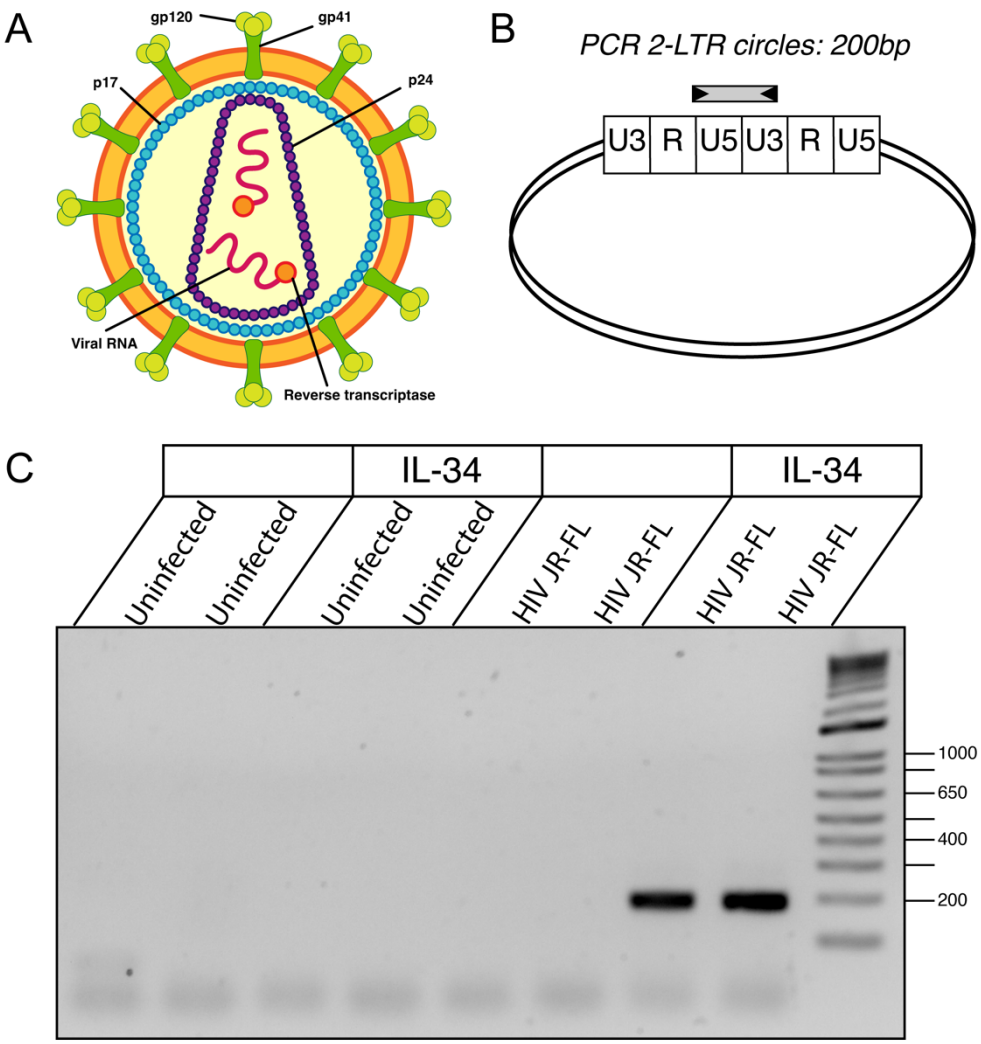

Supplemental Figure 2

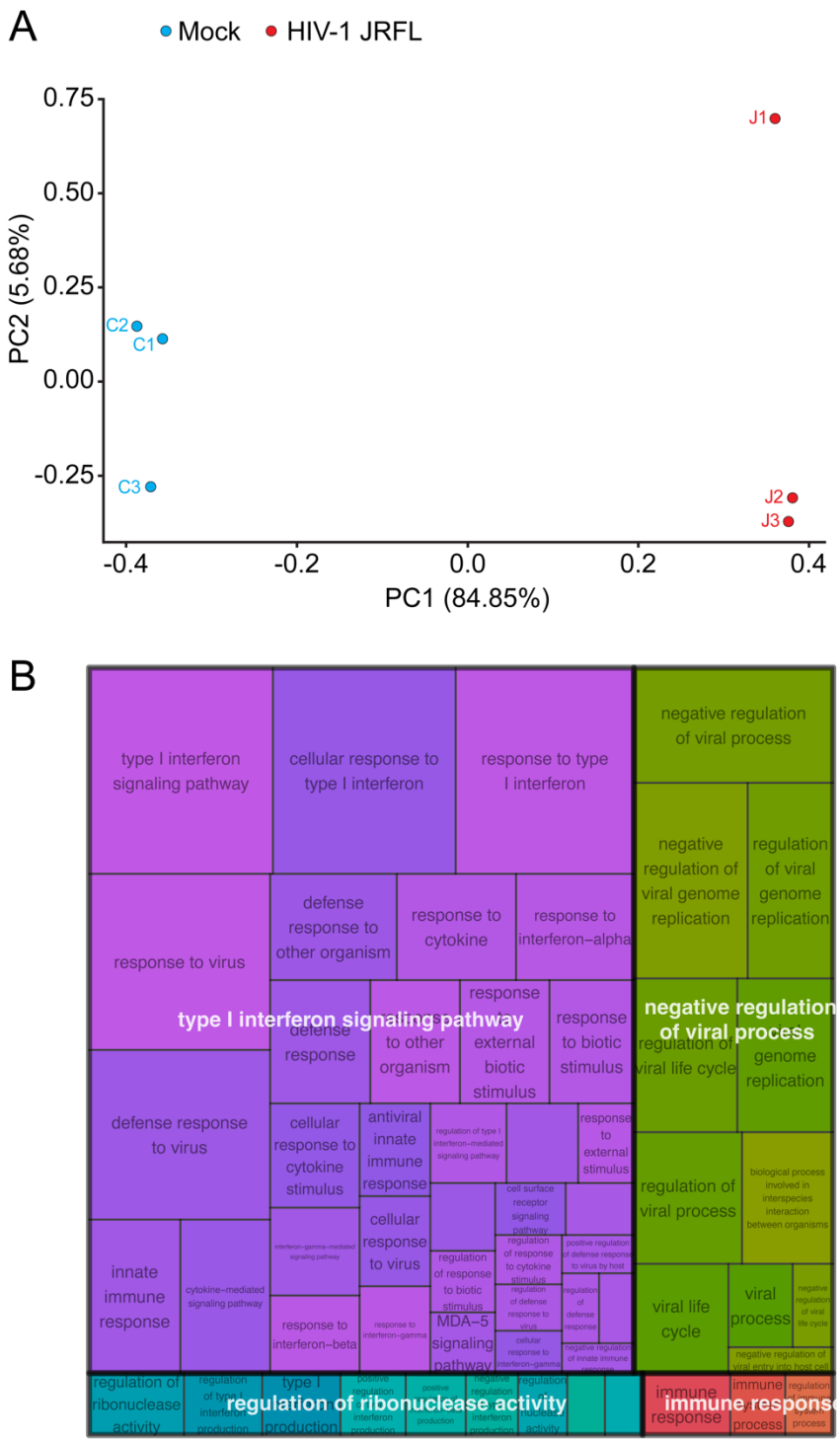

Supplemental Figure 3